SHALLOW SUBSURFACE GEOPHYSICAL APPLICATIONS IN ENVIRONMENTAL GEOLOGY

Field Guide and Conference Proceedings

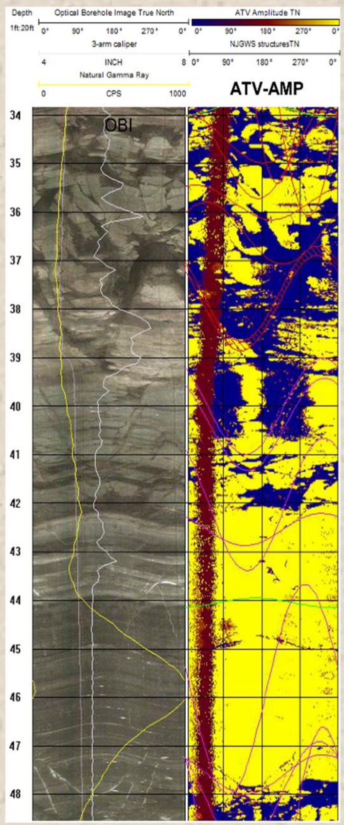

EDITED BY

Michael P. Gagliano

New Jersey Geological and Water Survey

and

Suzanne Macaoay Ferguson

PennJersey Environmental Consulting

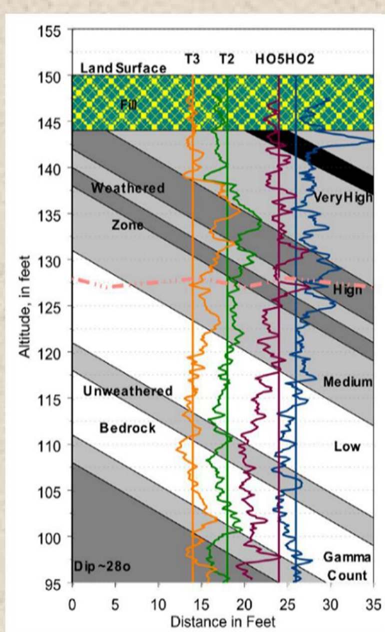

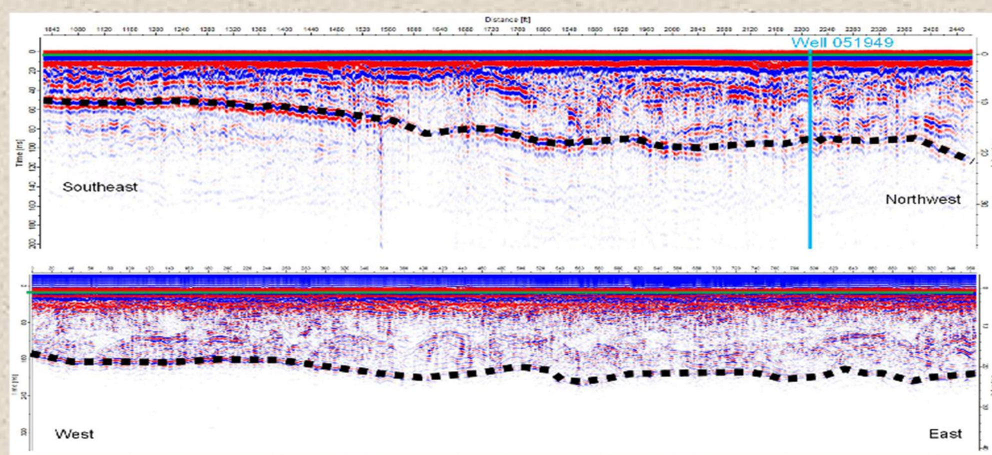

THIRTY-THIRD ANNUAL MEETING OF THE

GEOLOGICAL ASSOCIATION OF NEW JERSEY

OCTOBER 14-15, 2016

THE NEW JERSEY STATE MUSEUM
TRENTON, NEW JERSEY

TABLE OF CONTENTS

NJGWS Calibration and Flow Studies Using Heat-Pulse Flow Meter Model HFP-2293

Gregory C. Herman, Mark A. French, and Rachel M. Filo, New Jersey Geological and Water Survey

Chief James T. Boyle and coauthor Mark French oversees HFM system testing in the NJGWS garage. The HFP-2293 is positioned in the clear, 7.5-inch pipe to the right and setup for upward, low-flow testing.

Herman, G. C., French, M. A., and Filo, R. M., 2016, NJGWS calibration and flow studies using heat-pulse flow meter model HFP-2293, *in* Shallow subsurface geophysical investigations in environmental geology, Gagliano, M. P. and Macaoay Ferguson, S., eds., 33rd Annual proceedings and field guide of the Geological Association of New Jersey, Trenton, NJ, p. 18-48.

Introduction

A heat-pulse flow meter (HFM) is a geophysical sonde used to measure sub-vertical (axial) water-flow rates in water wells. It's ordinarily deployed in a static, non-trolling mode and works when a field operator triggers a heat-pulse to be released from a wire grid (Figure 1B) into a water column. Moving water will carry a heat pulse past one of two heat sensors (thermistors) that are housed within the sondes measurement chamber and situated at fixed distances (~ 2cm) above and below the heat source (Figures 1 and 2). The time it takes for the maximum amplitude of the heat-pulse to pass by a thermistor is the instrument-response time (IRT). An IRT is used to calculate axial flow rates (feet or meters per second or minute) using a mathematical equation that relates IRTs to flow as determined by calibration flow tests. Volumetric rates (gallons or liters per minute) are calculated by multiplying axial flow rates by the area of the borehole cross section, which is a function of borehole diameter. Ordinarily, the field technician records multiple firing-and-response cycles at various fixed depths to determine an average flow rate at each depth (Figure 2).

HFM technology was developed in the early 1980's and is in widespread use today for groundwater investigations involving open boreholes developed in fractured bedrock having discreet, permeable subsurface features (Hess, 1986; Hess and Paillet, 1990; Paillet, 1998). HFM technology is recognized in a New Jersey Department of Environmental Protection (NJDEP) procedure manual (NJDEP, 2005) and guidance document (NJDEP, 2012) as a geophysical instrument that can help identify discreet, permeable fractures and the nature of borehole cross flows in a well field. This information is helpful for characterizing and remediating groundwater pollution sites in fractured-bedrock terrain, but lingering issues have hampered quantitative use of HFM results to determine aquifer characteristics. For example, the manufacturer's design of the HFP-2293 restricts its use to low-flow measurements below ~1gpm and there has been little quality-assurance testing done on this model to see how it performs under varying hydraulic conditions resulting from changes in borehole-diameter, flow rates and directions. This report therefore summarizes a series of flow tests conducted by the NJGWS using a Mt. Sopris Model No. HFP-2293 subject to varying flow conditions and using different flow-diverter designs, two of which allow a percentage of the water column to bypass the sondes measurement chamber (Figure 1). Initial field tests in 2011 were run in cased sections of 6- and 8-inch diameter water wells while inducing upward flows at controlled flow rates ranging between 1.2 to 3.0 gallons-per-minute (gpm). A subsequent set of laboratory tests run in 2014 at the NJGWS facility used custom-built flow chamber s capable of sustaining uniform, bi-directional axial flows at rates between 0.01 and 8 gpm in vertical pipes of 5.5- to 7.5-inch diameters. This apparatus was used to test two HFP-2293 sondes and three different flow diverters, two of which allow a percentage of cross flows to bypass the measurement chamber. The test results were charted using MS Excel to derive flow-calibration curves for each diverter to use during subsequent field work in order to expand the HFP-2293 operational range and to increase its reliability. A MS Excel worksheet was also developed to aid in calculating flow rates in the field or office that factors in slight variations in borehole diameter. The test results show that instrument behavior is best represented using power functions that test at about 80% to 90% accurate at flow rates below ~8 gpm. Recommendations on deploying and using a Model 2293 HFM are made for using the customized bypass diverters and flow calculator based on past experiences.

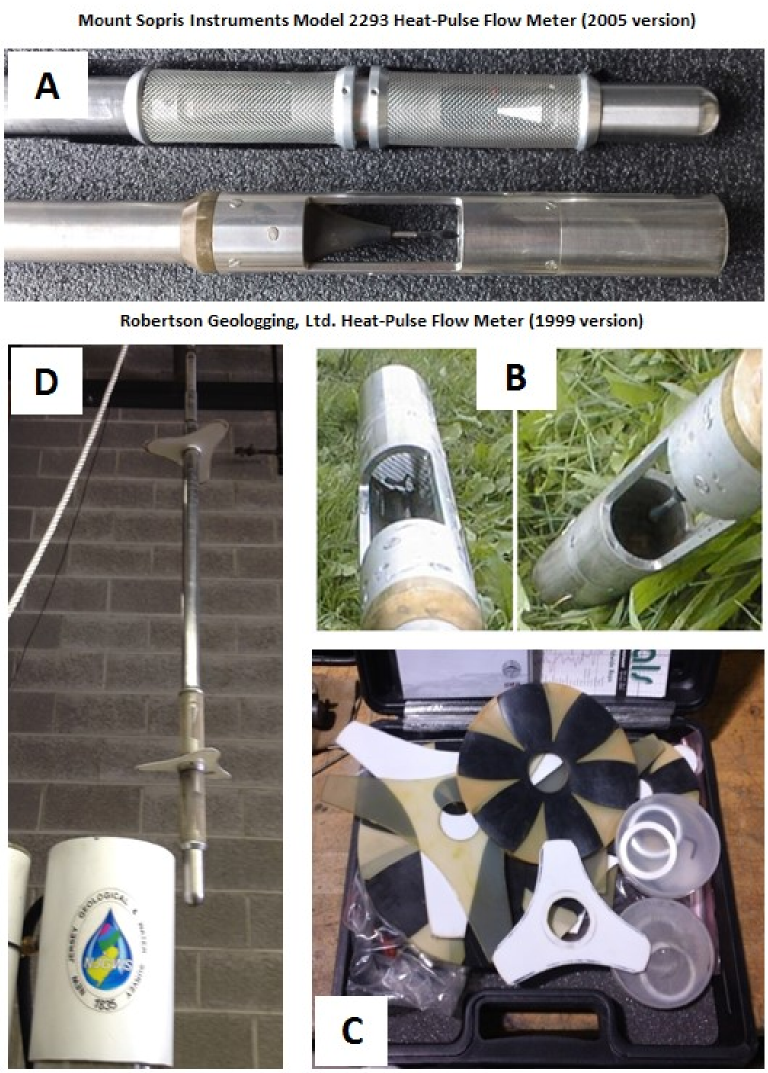

Figure 1: Photograph of the NJGWS heat-pulse flowmeter sondes and flow diverters. (A) Detailed views of the measurement chambers of two different sondes without flow diverters (C) attached. The Mt. Sopris HFP-2293 (top) includes screen guards covering two, lateral-entry ports into a close-ended measurement chamber. The Robertson Geologging model (bottom) has one lateral port and is open-ended on its bottom (B). The HFP-2293 standard deployment scheme uses the yellow (latex) and black (neoprene) flexible petals (C) that mostly seal the borehole annular space and divert nearly all cross flows through the instrument-measurement chamber. The Robertson tool was deployed using the two centralizers pictured in (D) that were also tested on the HFP-2293 for flow-rate measurements >1 gpm, the recommended threshold of the HFP-2293. A wire-grid heat source is pictured on the left side of photo (B).

Background

The NJ Geological and Water Survey (NJGWS) purchased a Mt. Sopris model number HFP-2293 flow meter in 2010 for use in characterizing fractured-bedrock aquifers in support of publicly funded groundwater investigations within the NJDEP. This instrument is part of a logging system that includes flow diverters to facilitate measuring in-situ groundwater-flow rates between ~0.03 to 1.0 gpm according to the manufacturer's product specifications. This is the second HFM system used by the NJGWS. The first was a Robertson Geologging, Ltd. system purchased in 1999 that was tested in the field to be about

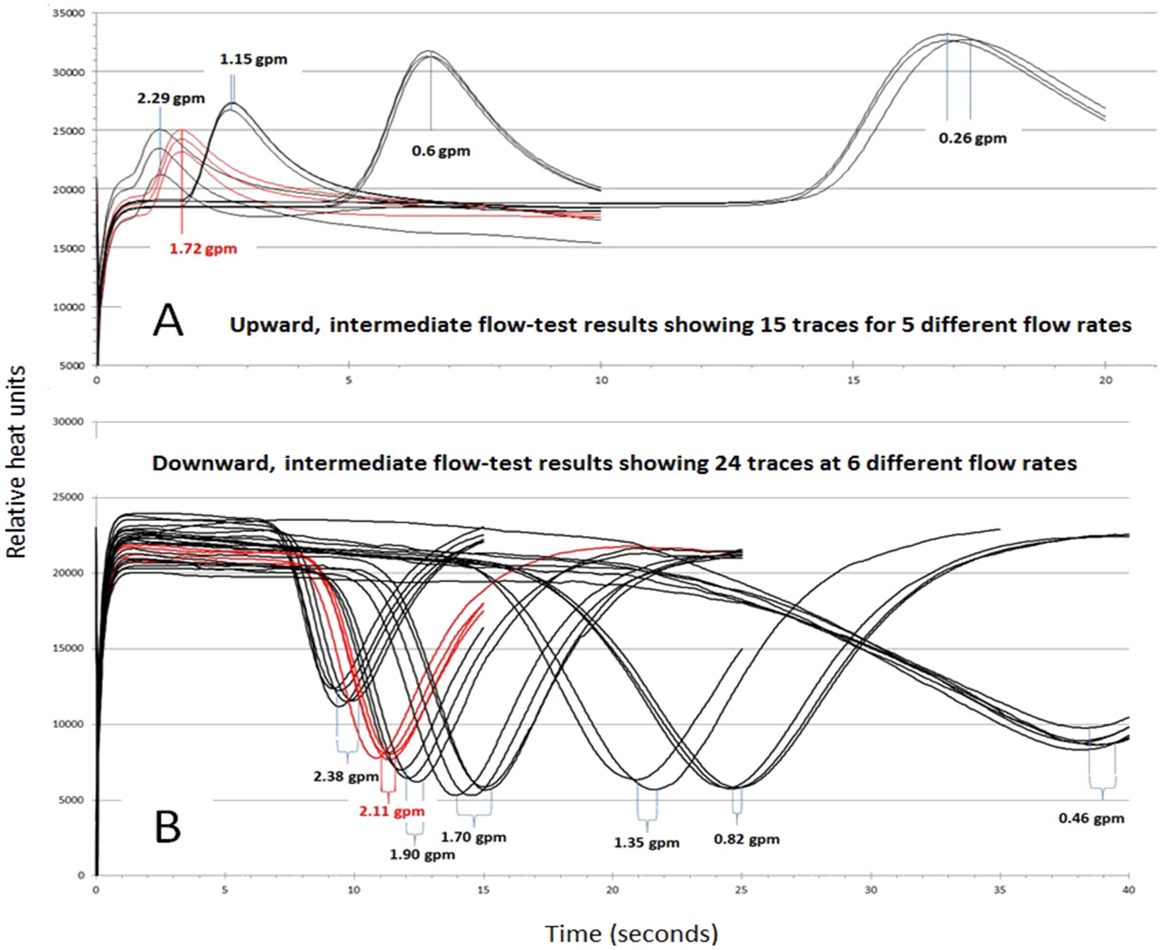

Figure 2: MS Excel scatterplots of instrument-response times (IRTs - x-axes) versus thermistor responses (y-axes) using relative thermal units. Note that upward flows (A) register upward deflections and downward flows (B) register downward deflections. Multiple readings were taken at controlled flow rates to derive average response times; these were then charted versus flow rates (gpm) to derive reference curves (Figure 3). The red traces are colored for clarity.

80% accurate when measuring cross flows ranging from 0.7 to 25.0 gpm in 6- and 8-inch diameter water wells drilled to depths ranging to about 500 ft. (Herman, 2006). That sonde was operated in a stationary, non-trolling mode and deployed with centralizers (1C) that partially restricted cross flows in the borehole but not the measurement chamber. The flow-chamber design of the Mt. Sopris sonde is similar to that of the Robertson one (Figure 1A), but the HFP-2293 is supplied with a set of flow diverters made of flexible, yellow latex and black neoprene (Figure 1C) that mostly seal the annual space between the lateral entry ports and channel cross flows through the sondes measurement chamber (Figure 1AC). Use of the tool in this manner provides measurements at low-flow rates (~<1.0 gpm), but cross-flow rates in water wells developed in bedrock aquifers in this region are an order of magnitude higher in places (Herman, 2010; 2006). Therefore, standard deployment methods for the HFP-2293 cannot solely be relied upon to gain results from the expected range of encountered cross flows in this region.

2011 Field Tests Using Customized Diverters for Borehole Cross Flows Exceeding 1.0 GPM

Field testing of the HFP-2293 began in 2011 for upward cross flows exceeding ~1.0 gpm using customized diverters that allow different percentages of water to bypass the instrument measurement chamber during testing (Figures 1C and D). As for the previous study using the Robertson HFM (Herman, 2006), these tests were only conducted for upward, axial flows at stepped-rates (Figure 3) controlled by a throttled water pump positioned above the flow meter in the water column. The calibration of downward axial flows wasn't done owing to the inconvenient arrangement of having the pump's discharge pipe rising through the section of borehole annular space being tested and thereby compromising the borehole hydraulics. These initial tests were conducted in steel-cased sections of 6- and 8-inch diameter wells located at the Stony Brook-Millstone Watershed Association well field in Mercer County, NJ. The wells are located near a pond and have shallow static water levels (wells 93 and 97 of Herman and Curran, 2010) with near-instantaneous recovery at low-flow rates.

For each test, the sonde was outfit with two tri-wing centralizers of Mt. Sopris design (Figure 1B). The translucent –yellow, plastic centralizers of tri-wing design provided with the sonde (Figure 1D) served as templates for duplicating the design using white, thin plastic cut from the bottom of a 5-gallon bucket (Figures 1C and 1D). One centralizer was positioned on the upper part of the sonde and the other was placed between the screen guards in the middle of the instrument's measurement chamber to restrict, rather than fully divert cross flows (Figure 1D). The HFP-2293 was submerged within two feet of the bottom of casing and at least 10 feet below a small submersible pump connected to a rheostat flow-rate controller at the surface. A series of steady-state pumping tests were run using stepped rates varying from 1.0 to 3.0 gpm and measured using a stopwatch to gauge the rate and volume of pump discharge into a 5-gallon graduated bucket. During each test phase, the sonde was fired multiple times to record a set of IRTs after achieving near-steady-state flow conditions at each pumping rate (Figure 2). Each set of test data were charted on scatter graphs using MS Excel with instrument-response times plotted on the x axis and flow rates plotted on the y axis (Figure 3).

Statistical regression curves were then derived for each test plot using MS Excel statistical functionality to produce the best mathematical formulae and reference curves for subsequent field use. As seen in the results of the earlier flowmeter tests with the Robertson system, power functions provide the most accurate regression statistics for the observed non-linear system responses in comparison to other standard statistical options included in MS Excel including polynomial, exponential, and logarithmic solutions. But despite employing these power-solution reference curves, subsequent field use of the HFP-2293 under low-flow conditions sometimes resulted in significant discrepancies when compared to flow rates determined with other methods such as timing the recovery of the static water table in well casing after pumping the well. We therefore set out to further test and customize the HFP-2293 in order to expand its operating range and to better understand its limitations. To do this we designed (Figure 4) and built (Figures 5 and 6) customized flow chambers using 6 foot lengths of clear piping having 5.5- and 7.5

inch diameters. The HFP-2293 was then outfit with three different sets of flow diverters (Figure 7), two of which allow varying amounts of flowing water to bypass the sonde in order to test the new system under varying hydraulic conditions.

2014 Laboratory Tests Using a Custom-Built Flow Chamber and Flow Diverters

Prior to 2014, field calibration of both HFM systems was only done for upward axial flows in shallow water wells because of the aforementioned restrictions that compromised testing of downward-directed flows in the field. The NJGWS flow chamber therefore provides the means to more thoroughly test flow meters in pipes of varying diameters, flow rates and directions. The apparatus frame was constructed using ¾-inch plywood that is built to receive upright-standing pipes ranging between 5.5 and 8-inch diameters (Figure

A

2011 FIELD TESTS RESULTS

4-inch Diameter

TIME seconds	RATE gpm
2.2	3.00
2.4	2.50
3.1	2.00
3.8	1.50
4.4	1.25
5.2	1.00

6-inch Diameter

TIME seconds	RATE gpm
6.7	2.90
7.9	2.50
9.6	2.25
10.8	2.00
14.1	1.70

8-inch Diameter

TIME seconds	RATE gpm
8.5	3.02
8.9	2.50
11.0	1.87
14.7	1.67
20.7	1.22

B

2014 FLOW CHAMBER RESULTS

5.5-inch Diameter TIME seconds	5.5-inch Diameter RATE gpm	7.5-inch Diameter TIME seconds	7.5-inch Diameter RATE gpm
22.90	0.86	16.80	1.72
23.10	0.86	17.75	1.72
23.25	0.86	18.70	1.72
23.44	0.86	20.70	1.72
22.90	0.86	23.95	1.72
19.16	1.00	16.65	1.72
19.16	1.00	14.08	2.50
19.00	1.00	13.56	2.50
19.16	1.00	13.25	2.50
8.35	1.54	7.70	3.40
8.80	1.54	7.80	3.40
9.10	1.54	3.83	5.80
9.00	1.54	4.20	5.80
4.15	2.50	3.75	5.80
4.25	2.50	4.30	5.80
4.25	2.50	4.00	5.80
2.75	3.33	4.25	6.70
2.70	3.33	3.95	6.70
2.70	3.33	3.56	6.70
1.80	4.70	3.40	6.70
1.80	4.70	3.65	6.70
1.80	4.70		
1.15	6.90		
1.15	6.90		
1.15	6.90		

F

YEAR	HFM	Pipe diameter (in)	MS Excel optimum regression soluiton
2005	Robertson	4 inch	Q = PRODUCT(6.2*(POWER(IRT,-0.8)))
2011	Mt. Sopris	4	Q=PRODUCT(7.586*(POWER(IRT,-1.222)))
2011	Mt. Sopris	6	Q = PRODUCT(10.842*(POWER(IRT,-0.703)))
2011	Mt. Sopris	8	Q = PRODUCT(19.42*(POWER(IRT,-0.922)))
2014	Mt. Sopris	5.5	Q = PRODUCT(6.971*(POWER(IRT,-0.676)))
2014	Mt. Sopris	7.5	Q = PRODUCT(17.95*(POWER(IRT,-0.786)))

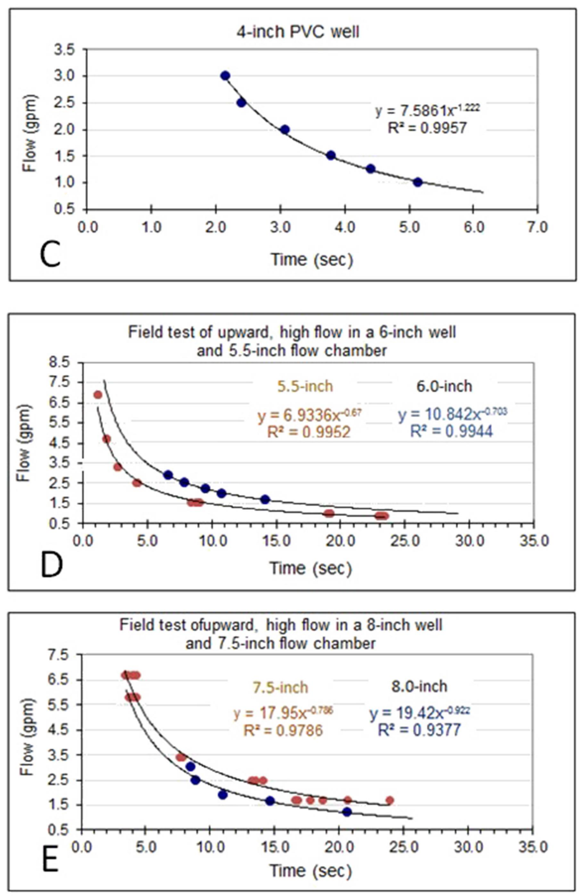

Figure 3: Results of 2011 field- and 2014-laboratory testing of the HFP-2293 at borehole flow rates of 0.5 to ~8 gpm using the customized bypass diverter pictured in Figure 1D. The 2011 initial tests were only run for upward flows. Laboratory test results run in 2014 in 5.5- and 7.5-inch diameter pipes are summarized in (B) and plot alongside the earlier results in (D) and (E) for comparison. The sequence of statistical regression curves summarized in (F) summarize the statistically optimum power functions derived from the respective tests with correlation coefficients (R^2) exceeding 0.93 and mostly above 0.97(C-E). See text for further discussion.

4 to 6). For these tests, it was supplied with two 6-foot long, clear acrylic pipes having ¼-inch thick walls and 5.5- and 7.5-inch inside diameters (ID). The pipe outside diameters are the same as the ID of 6- and 8-inch schedule 40 PVC pipes, so the clear ones fit snugly inside cut PVC pipe segments. Each acrylic tube is set and glued inside a short segment of schedule 40 PVC pipe that was capped, drilled, and tapped to receive 1-inch galvanized pipe nipples as flow ports to connect supply lines and discharge hoses (Figure 5A). Pipe nipples with garden-hose adapters were set into the upper PVC pipe segment for inflow or outflow ports depending upon the desired flow direction (Figure 6A). Larger-diameter ports were also plumbed into the PVC pipe segments using 1¼-inch pipe nipples or threaded pipe adapters to connect larger pipes when testing higher flow rates (Figure 5C). The apparatus was connected to either to a municipal water-supply line (Figure 5A and B) or run through a constant-head bath to establish flows in the 0.01 to 10.5 gpm range with input lines connected at the top or bottom depending upon the

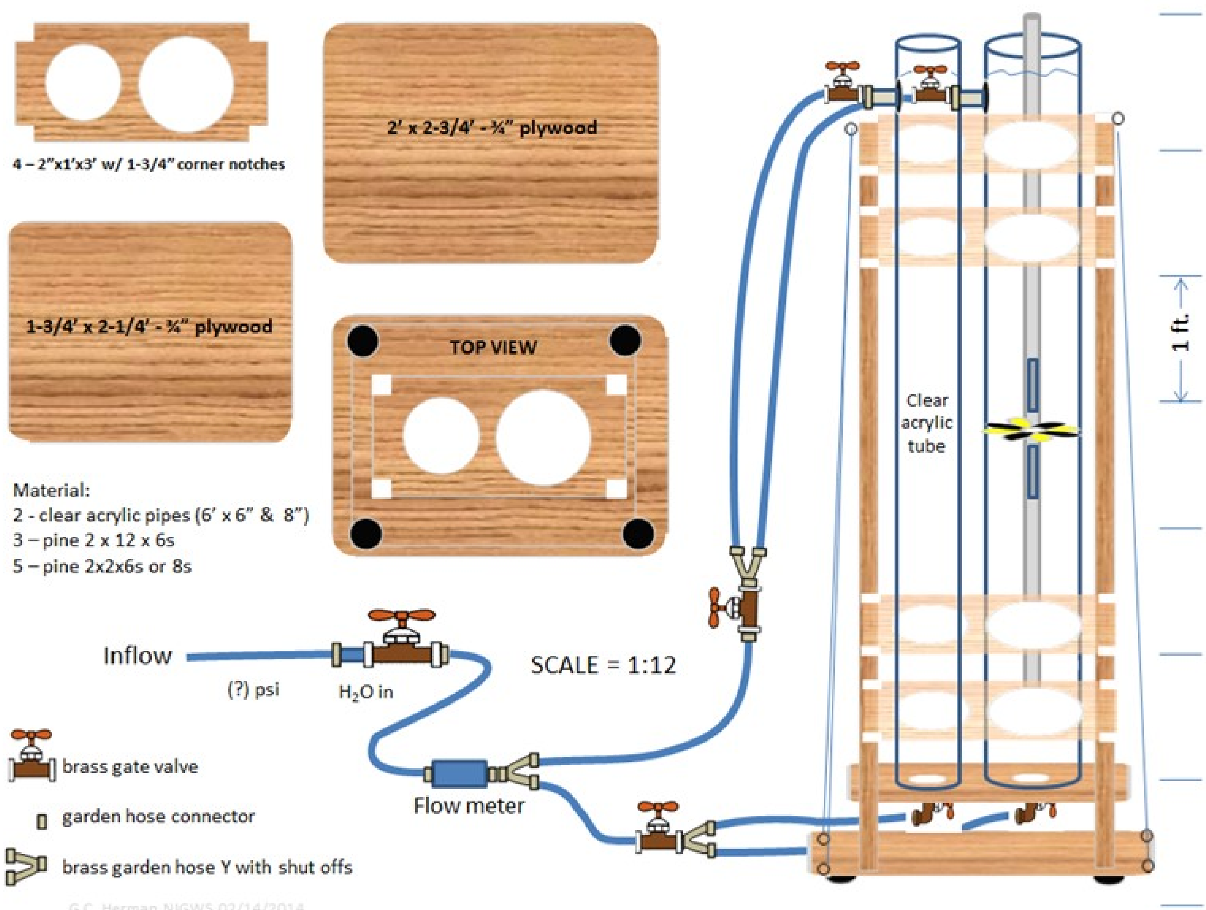

Volume of water in pipe (V) with water column (h)

6" V = 1.47 h, 8" V = 2.81 h	1 gallon of water = 8.342 pounds
6 in. volume = 1.47 gal/ft x 6 ft = 8.82 gal	6 in. weight = 73.57 psf at bottom (0.51 psi)
8 in. volume = 2.81 gal/ft x 6 ft = 16.86 gal	8 in. weight = 141.96 psf at bottom (0.985 psi)

Figure 4: The schematic design of an upright-standing apparatus housing pipes with standard water-well diameters that can mimic sub-vertical (axial) cross-flows in open boreholes.

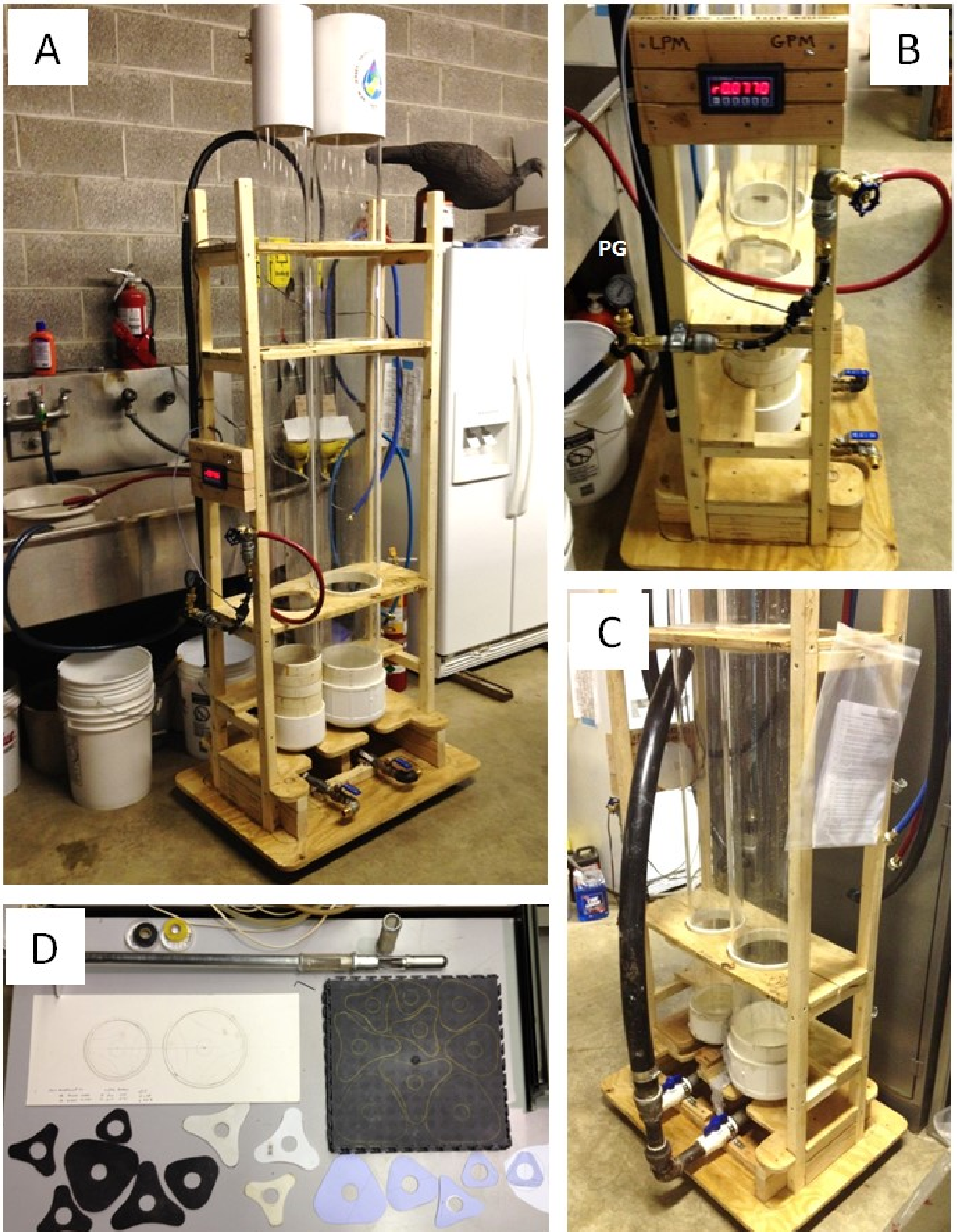

Figure 5: The HFP-2293 was tested using a custom-built flow chamber (A to C) and flow diverters of three different designs (D). The plywood frame holds the pipes upright and can be disassembled for pipe removal, modification, or substitution. As depicted when facing the front, the left side houses 5.5 to 6-inch (outside diameter or OD) pipes and the right side holds 7.5 to 8-inch OD pipes. An in-line pressure gauge (PG in photo B) and an electronic, digital flowmeter (A and B) provide monitoring points during testing. The flow diverters (5D) were cut from flexible, 1/4-inch thick, black-rubber floor matting (right side of D) using the blue-paper templates (lower right D) cut from a printed CAD design. Also note the lower screen guard is off the HFP-2293 in the upper right of photo D. The CAD file is available for free download as part of this report (www.ganj.org/2016/2016_NJGWS_HFM-2293_Flow_diverters.skp).

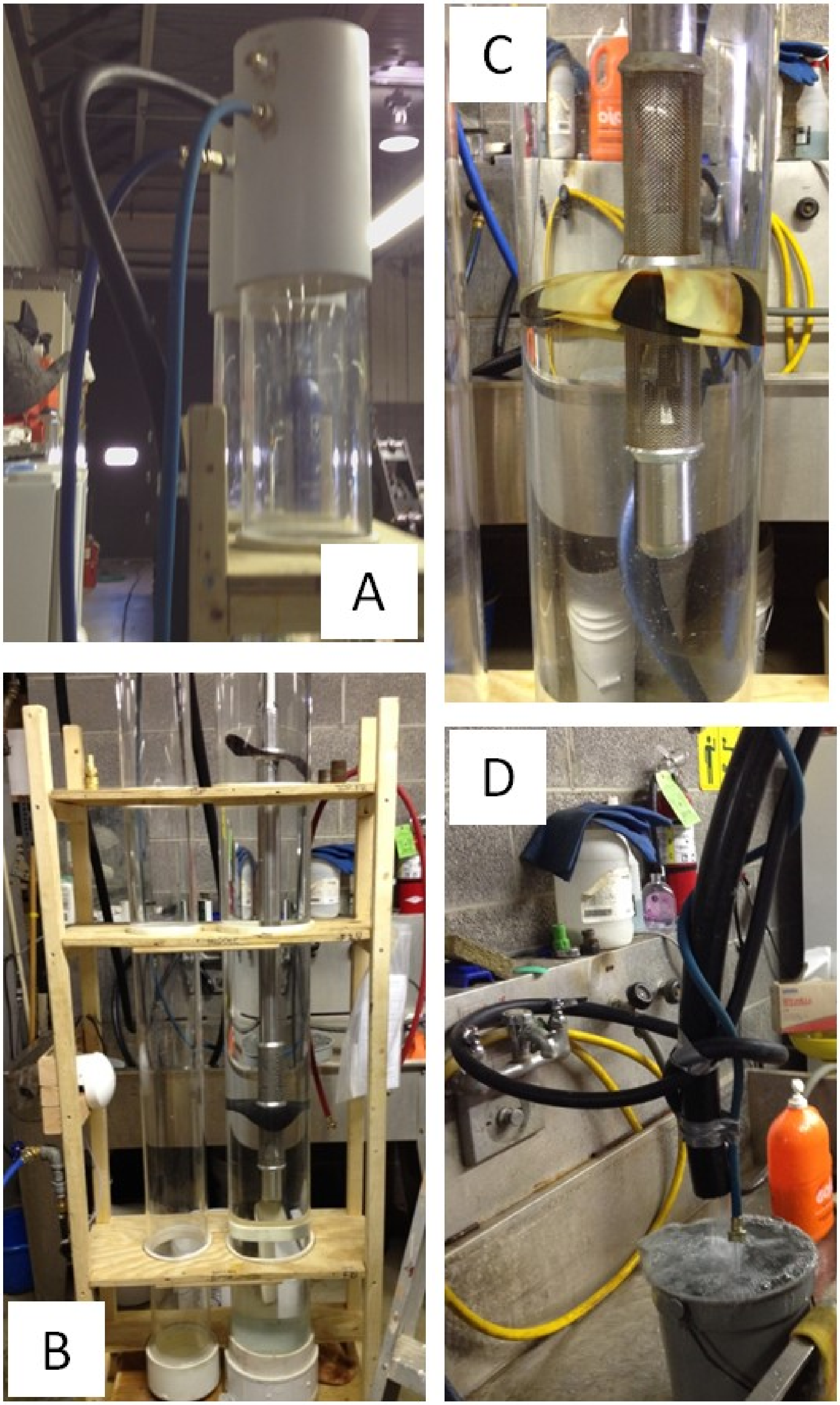

Figure 6: Photographs detailing the three deployment schemes tested in 2014 at the NJGWS lab (garage). Designs for low- (C), intermediate- (B), and high-flow (Figure 1D) rates were tested. The low-flow scheme is the default HFP-2293 deployment scheme of Mt. Sopris design. The other two are the NJGWS customized bypass diverters that allow a percentage of cross flow to bypass the sondes' measurement chamber (Figure 7).

desired flow direction. The bath is a 250-gallon plastic water tank sitting on a table in a loft over the flow chamber (Figure 8). A standard water-pressure gauge was attached to the input line using a T-connector with a shutoff valve (Figure 5B) to monitor water-pressures that fluctuated between ~15 to 50 pounds-per-square inch when connected to the municipal water-supply line. This line was used to generate flow rates greater than 1.0 gpm. An electronic flow meter was purchased and placed into the input line to monitor flow rates. Each chamber is therefore outfit with upper and lower flow ports in a plumbing system that provides either upward or downward axial flows at controlled flow rates ranging from about 0.01 to 8 gpm (Table 1). A series of flow tests were run using the HFP-2293 sonde with flow diverters of all three

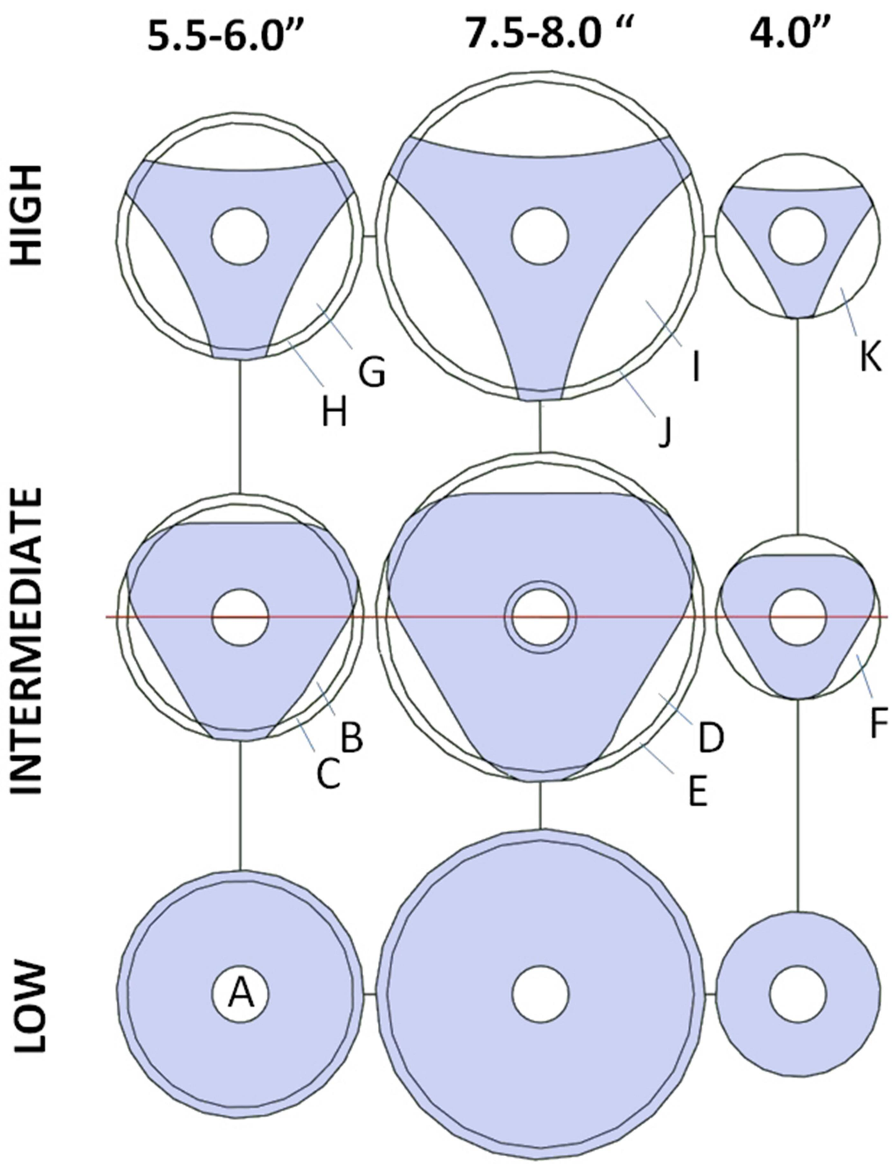

Diverter segment	Area Inches^2
A	1.31
B	3.31
C	3.21
D	6.91
E	4.63
F	5.53
G	9.06
H	3.65
I	21.91
J	5.20
K	5.53

Figure 7: SketchUp Make software (Trimble, Inc.) was used to design two passing-flow diverters covering high- and intermediate-flow rates. The diagram and accompanying table detail the total area of the borehole cross section that is open to flow using each respective design (www.ganj.org/2016/2016_NJGWS_HFM-2293_Flow_diverters.skp).

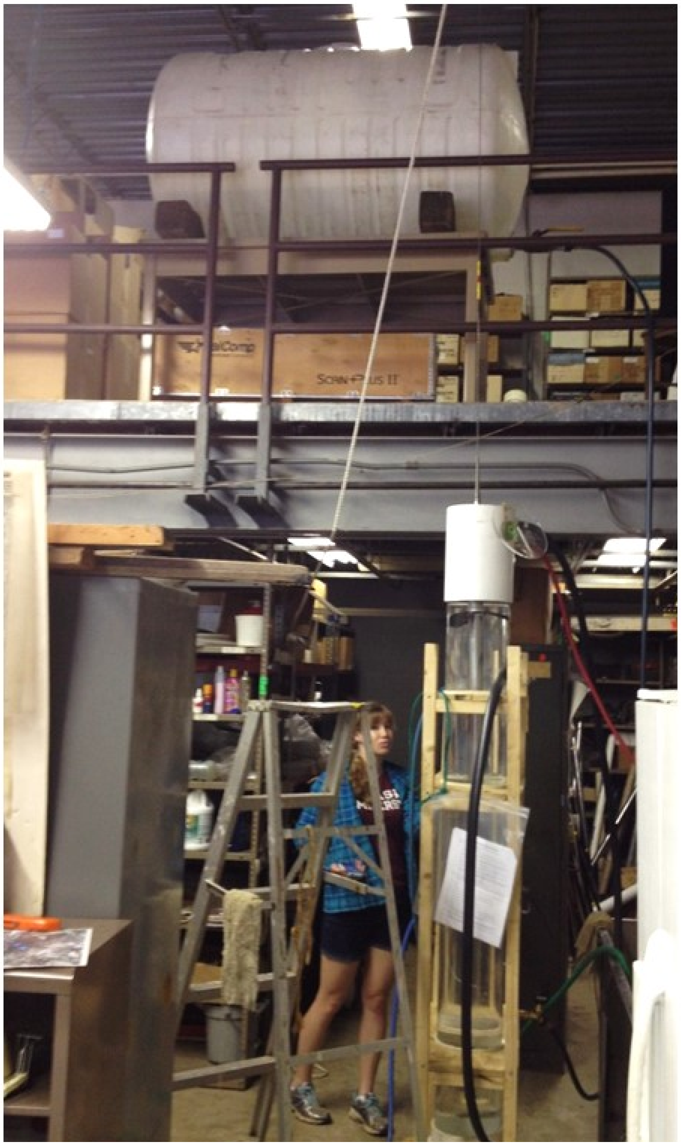

Figure 8: A 250-gallon plastic tank lofted about 8-ft above the testing apparatus provided a steady water supply needed for low-flow testing. Ms. Rachel Filo attends to the flow apparatus during testing.

designs (Figures 5D, 7 and 9) and variable rates of upward- and downward axial flows. All test results are tabulated as Appendix A and chartered as scatter plots in Figures 10 to 12. The Mt. Sopris diverters used for the low-flow tests are constructed of soft, yellow-and-black rubber formed into overlapping petals (Figures 5D, 6C, and 9D). The Mt. Sopris translucent yellow, plastic, tri-wing centralizer was used as a template for the high-flow bypass diverter (Figures 1C, 1D, 5D, 11 and 12C). A second bypass diverter was designed that provides less bypass area (Figure 7) and therefore an 'intermediate' range of flow rates. The customized flow diverters were designed using Trimble Inc. SketchUp Make software and cut out of stiff, but flexible, ¼-inch-thick rubber matting marketed as trafficMASTER Utility Floor Tiles product number 615 904 (Figure 5D). The CAD file of the custom-designed bypass diverters is available for download from the GANJ web site as noted in Figures 5 and 7. The two customized flow diverters were tested at high (>0.9 to <7.0 gpm) and intermediate (>0.2 to 20 gpm) flow rates (Figures 11, 12B, 12C, and 13). The 4-inch designs (Figure 11) have not been tested yet.

A second HFP-2293 was temporarily loaned to us by Princeton Geoscience, Inc. during testing at intermediate flow rates in order to provide a comparison of flow-test responses for the same model sonde. Two sets of examples gained from these tests are charted in Figure 14 to illustrate how IRTs can vary for various flow rates and directions. As found in the prior HFM calibration study (Herman, 2005) all charted test results are best represented using power functions that have regression coefficients (R^2) exceeding 0.97 (Figure 8 and Table 1).

Table 1: Summary of test results and instrument-response time-to-flow rate equations derived for use with the HFP-2293 flowmeter

Equation	Power-equation derived using MS Excel scatterplots	Borehole diameter (in.) and flow scheme	R^2	Volumetric flow range		Response time
				gpm	lpm	sec.
2	$y = 00.405\ x^{-1.098}$	5.5 Low down	0.99	>0.01 <0.40	>0.01 <0.40	>1.8 <32.0
3	$y = 00.467\ x^{-1.174}$	5.5 Low up	0.99			
4	$y = 02.278\ x^{-0.724}$	5.5 Intermediate down	0.97	>0.20 <2.00	>0.01 <0.40	>1.5 <42.0*
5	$y = 02.631\ x^{-0.799}$	5.5 Intermediate up	0.99			
6	$y = 05.899\ x^{-0.536}$	5.5 High down	0.99	>0.90 <7.00	>0.01 <0.40	>1.0 <24.0
7	$y = 06.419\ x^{-0.640}$	5.5 High up	0.99			
8	$y = 00.503\ x^{-0.965}$	7.5 Low down	0.99	>0.02 <1.00	>0.01 <0.40	>0.9 <21.0
9	$y =0\ 1.356\ x^{-1.220}$	7.5 Low up	0.93			
10	$y = 03.361\ x^{-0.541}$	7.5 Intermediate down	0.99	>0.30 <3.00	>0.01 <0.40	>1.8 <32.0
11	$y = 05.024\ x^{-0.866}$	7.5 Intermediate up	0.99			
12	$y = 11.301\ x^{-0.556}$	7.5 High down	0.98	>1.50 <8.00	>0.01 <0.40	>1.8 <32.0
13	$y = 17.950\ x^{-0.786}$	7.5 High up	0.98			

Comparison of Mt. Sopris and NJGWS Low-Flow Calculations

The power functions derived from laboratory testing at low-flow rates were next compared to flow values obtained using the Mt. Sopris MatrixHeat (ver. 3.3) software (Figure 14). The flow solution used in this software uses a 2nd-order polynomial that is modified form of the quadratic equation to approximate the observed, non-linear nature of the instrument-response time (IRT) to flow-rate responses (Figures 8-10):

***Eq. 1**: Flow (Q) = K1/DT + K2/DT²*

$$\text{Flow}\ (Q) = K1/DT + K2/DT^2$$

where K1 and K2 are constant values derived using tests conducted at low and high flow rates in a laboratory flow chamber at Mt. Sopris Instruments, Inc.

Each HFP-2293 is calibrated before shipping at the Mt. Sopris office in an upright-standing apparatus including a 6-inch-diameter clear-acrylic pipe. Calibration readings at both low- and high-flow rates are gathered and recorded on an 8.5x11" certificate of calibration included in the operator's manual with the most recent calibration results for the NJGWS tool included in Table 2. Fred Paillet of the US Geological Survey provided us proof of this method in a written communication dated January 7, 2015. The derivation uses six steps (a. to f. below) to calculate the respective K values for upward and downward

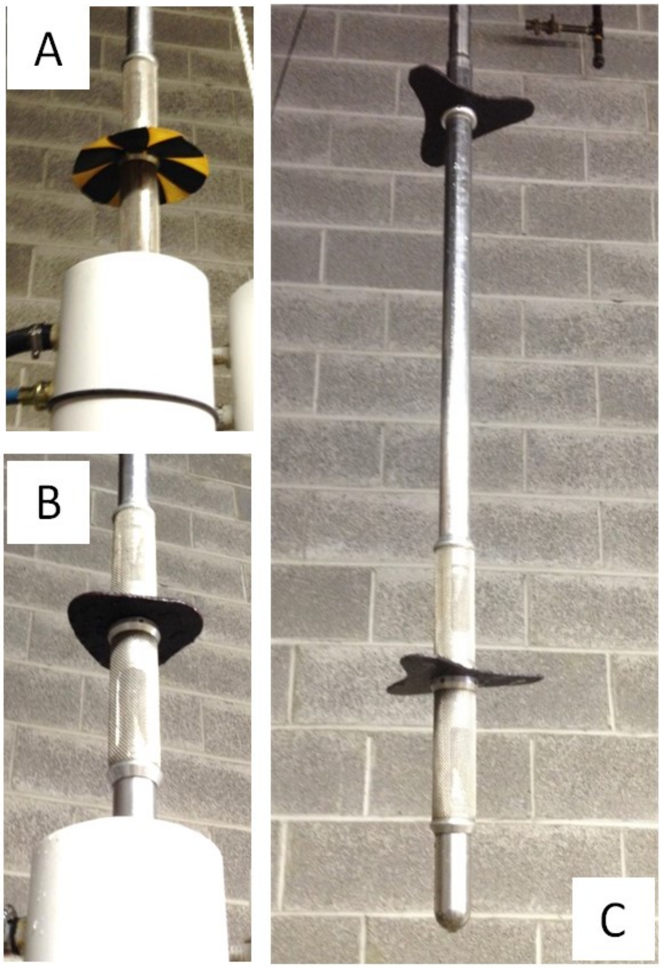

Figure 9: Photographs detailing the low (A), intermediate (B) and high flow-rate (C) deployment schemes tested for field use.

flow.

a. Assume $Q = AX^2 + Bx + C$ with X= the inverse of the pulse travel time (T) or $X = 1/T$

b. The variable C can be set to 0 because Q = 0 for very large values of T.

c. The calibration results for low and high flows in a given direction give a coupled set of equations:

Eq. 14 $Q_{LF} = A_{LF}X^2+B_{LF}X$,

and

Eq. 15 $Q_{HF} = A_{HF}X^2+B_{HF}X$

d. By letting K1= B and K2 = A, then solving for A and B using the calibrated flow-vs.- time responses in Table 2 for UPWARD flow:

$0.03 = 0.01A + 0.10B$, and

$1.0 = 2.0408A + 1.4286B$

Rearranging and factoring Eq. 2 gives:

$0.01A = 0.03 – 0.10B$ or $A = 3.0 – 10.0B$

e. Substitute A = 3.0 - 10.0B for A in Eq. 3, and by rearranging to solve for B:

$1.0 = 2.0408 (3.0 – 10.0B) + 1.4286B = 6.1224 – 20.4082B + 1.35B = 6.1224 – 21.7582B$

Therefore: **B (or K1) = = 0.2814**

f. Substituting B = 0.2814 into Eq. 2 to solve for A:

$0.03 = 0.01A + 0.1 (0.2814)$ or $0.01A = 0.03 – 0.02814 = 0.00186/.01$

Therefore: **A (or K2) = 0.1860**

This process is repeated using the downward flow parameters to derive the downward K value in the same manner (Table 2).

Table 2: 08/02/2014 Mount Sopris calibration results for the NJGWS probe, HFP-2293 SERIAL NO. 5006

DIRECTION	LOW FLOW				HIGH FLOW			
	gpm	T (seconds)	1/T	$1/T^2$	gpm	T (seconds)	1/T	$1/T^2$
UP	0.03	10.00	0.1000	0.0100	1.00	0.70	1.4286	2.0408
DOWN	0.03	9.75	0.1026	0.0105	1.00	0.70	1.4286	2.0408

Figure 10 summarizes the derived set of power functions that returned the lowest statistical errors, and shows that the manufacturer's method offers a close match to the control rates only for upward, axial flows in ~6-inch boreholes. These tests also show significant departures in ~ 8-inch diameter boreholes between upward- and downward-flow responses (Figure 14 B). This is elaborated below in the concluding section below.

MS Excel Worksheet for Calculating Flow Rates Based on HFP-2293 Response Times, Including Linear Functions for Adjusting Flow Rates Based on Borehole Diameter for Passing-Flow Measurements

A comparison of test results acquired in the field in 2011 and the laboratory in 2014 provided the basis for including a linear 'caliper' function in the flow-calculation worksheet to adjust calculated flow rates based on variations in borehole diameter (caliper) when deploying the tool at intermediate to high rates of flow in ~6- to 8-inch diameter wells (Figures 6, 9, and 14). The method uses a linear function derived from conducting tests in both 7.5- and 8-Inch wells that relates an ideal percentage of passing-flow area (PFA) versus the borehole diameter (Figure 9). Each resulting function detailed in Figure 13 is programmed into the MS Excel flow-calculator worksheet as part of the workbook accompanying this report.[1]

The acquisition of HFM IRTs and calculation of flow-rates from using the custom flow diverters is thus,

1) Calculate flow rates based on IRTs using the appropriate regression (power) curve derived for the respective 5.5 (PWR5.5) or 7.5-inch (PWR7.5) pipes, and then

2) Modify the calculated flow rate using a caliper factor (CF) for each case (5.5-6.2 or 7.5-8.2), using the linear equations (Figure 11) derived from charting the percentage of PFA and the borehole diameter (CALIPER).

[1] The MS-Excel workbook for use with the NJGWS custom flow diverters is available to download at the following URL: www.ganj.org/2016/2016%20MS_HFM_2293_NJGWS-diverters.xls.

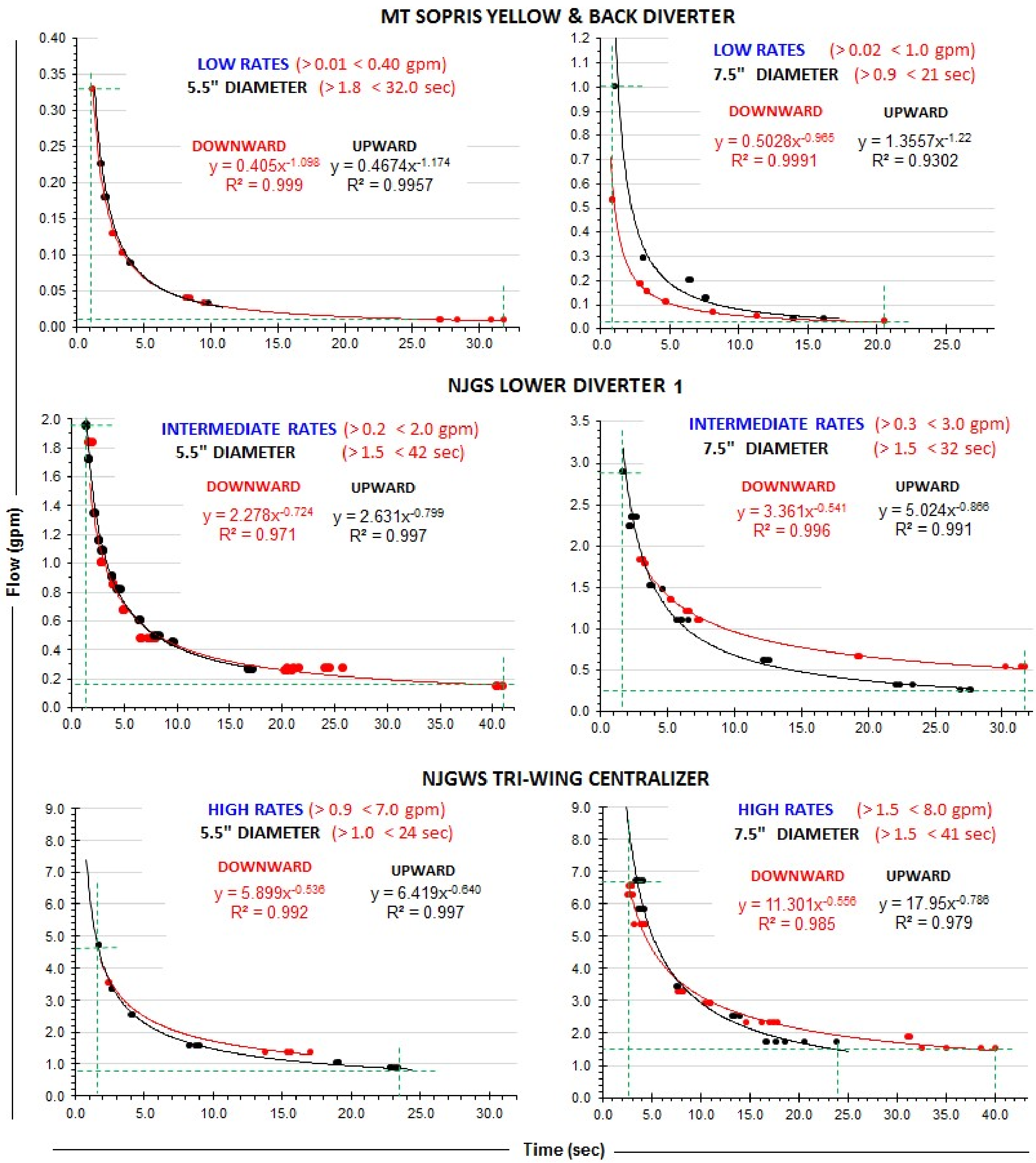

Figure 10: MS Excel charts of IRTs (seconds) versus flow rates (gpm) for the twelve different flow-test experiments needed to initially characterize upward and downward cross flows using two different pipe diameters (5.5- and 7.5-inch) and three deployment schemes covering 'low', 'intermediate', and 'high' rates. The results of downward-directed flow test are charted using red points and lines whereas upward-directed ones are colored black. The time- and flow-rate limits of each test are marked using green-dashed lines on each chart, and mathematical equation for each of the best-fit regression trends are summarized, and repeated in Table 1 and for use in the MS Excel rate calculator (Figure 15).

Table 4 summarizes typical errors that one can expect to encounter when using this customized setup and basing the error of accuracy on the difference in observed and calculated flow rates in the 6- and -inch diameter wells.

Notes and Discussion

This study set out to more thoroughly test the capabilities and limitations of a HFP-2293 system and in the course, we fabricated a solution to expand the instrument's operating range to cover borehole cross flows at rates between ~1.0 to 8 gpm. These applications are currently being field tested and await subsequent reevaluation and refinement. But for now, we now have a better understanding of some of the system limitations and pitfalls of using the standard operational method, and we provide an alternative way of deploying this system and calculating flow rates to achieve higher accuracy from using the MS Excel flow-calculator worksheet derived from both field and laboratory testing. But more work could attain

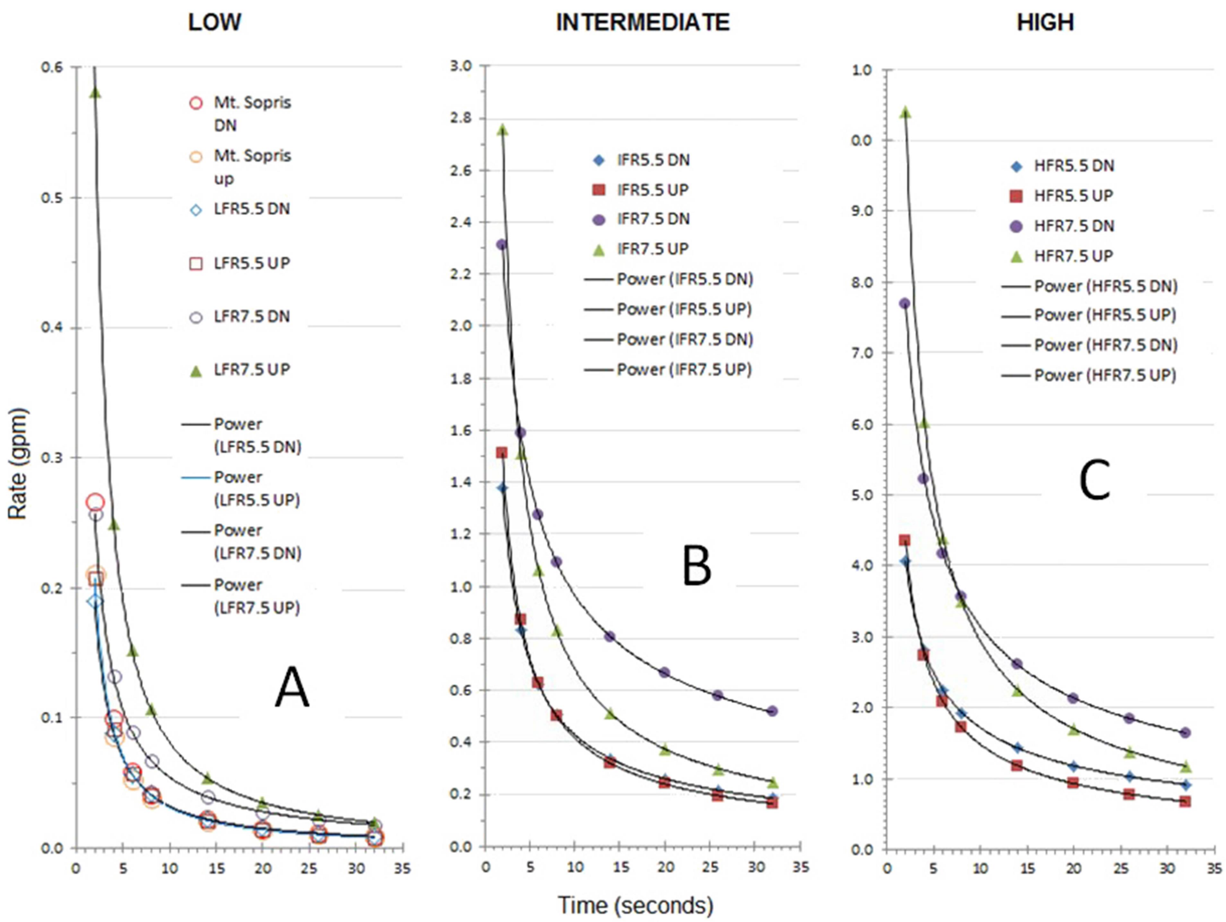

Figure 11: Charted test results from testing three diverter schemes using the flow chambers. Low-flow used the Mt. Sopris black-and-yellow full diverters whereas intermediate- and high-rates used the customized diverters that allow a percentage of flow to bypass the HFP-2293 measurement chamber. Table 2 summarizes the respective flow ranges and testing statistics.

even better results. For example, the flow chambers are capable of being outfitted with standard 4, 6, and 8-inch PVC schedule 40 pipes to compare the results obtained using the 5.5- and 7.5-inch clear-acrylic ones. The clear pipes were used first in order to help position and effectively seat the diverters and for visually inspecting the placement and seating of the instrument-measurement chamber as far from flowing ports as possible in order to obtain the best test results. More tests can be run to test axial flows in slightly larger-diameter pipes to confirm the earlier field tests and refine the methodology more. Below are some operational and test notes that may be useful when using HFM systems and discussion of some key test results.

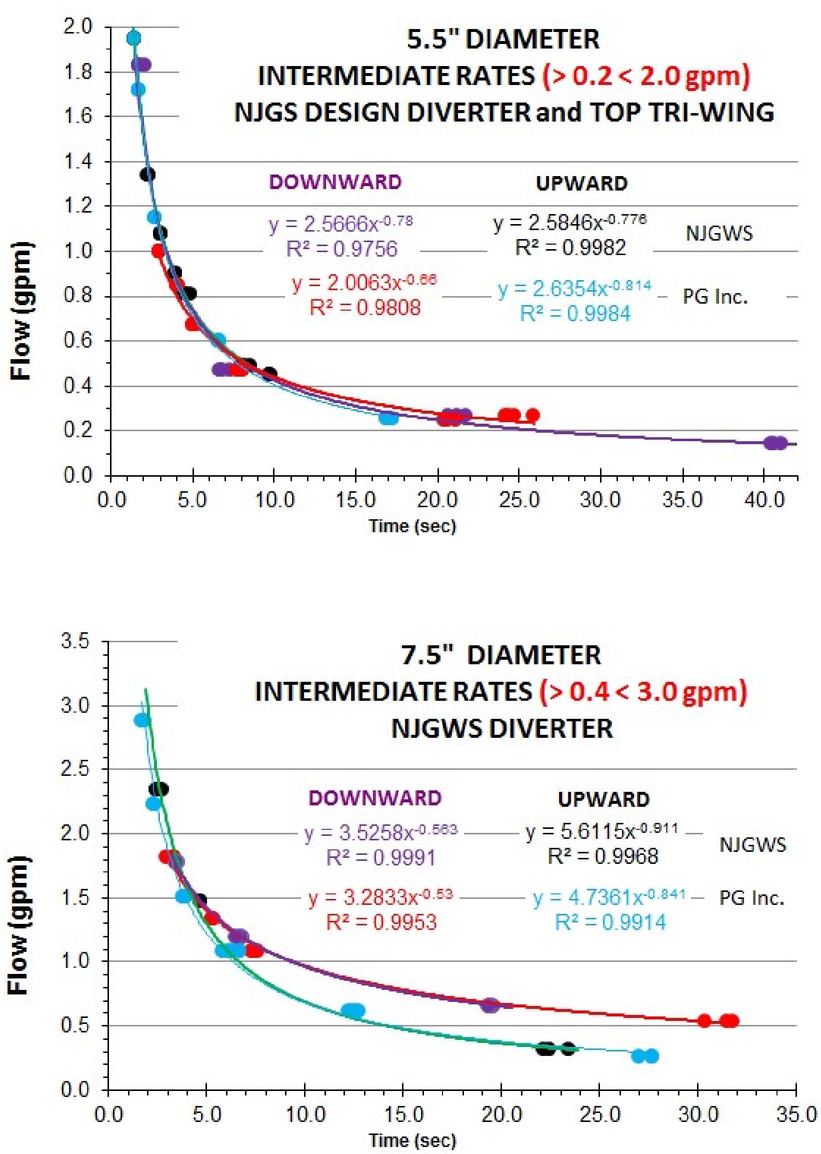

Figure 12: HFP-2293 tests results from using two different models under the same laboratory conditions. Flow responses in both upward and downward directions for the two tools for the intermediate- and high-flow schemes were nearly identical.

Figures 8A and 9A show that at low-flow rates below 1 gpm in 5.5 to 6-inch wells while and using the fully diverted setup, that directional flow behavior is very similar such that a single power curve could be used to attain a IRT-to-flow rate conversion that is over 95% accurate for either flow direction. Moreover, Table 3 and Figure 14 show that relying on the manufacturer's software to determine flow rates only achieves about 80 to 90% accuracy of flow determinations, especially depending upon the flow direction. At higher flow rates using the passing-flow deployment schemes, flow responses show even more separation depending upon flow direction such that two reference curves are needed to address each deployment scheme in order to achieve the most accurate results (Table 4). In general, this simply shows that a heat pulse is transmitted upward at a comparatively faster rate than a downward-directed one. This makes sense thermodynamically with regard to heat rising by convection through a fluid. However, this tendency is reversed for an unknown reason in the 5.5 to 6-inch diameter pipes when fully diverted (Figure 8B). Another notable test result is that the trend lines for intermediate- to high-flow rates tend to cross over at various points (Figures 8D, 8F, 9B and 9C). More work is needed in order to better understand these relationships. Figure 10 and Table 4 shows that the larger-diameter pipes resulted in significantly different IRTs registered in different directions for the same flow rates, and why it is therefore necessary to calibrate a HFM system for use in larger- and smaller-diameters wells other than the more common 5.5- to 6-inch. This also serves as a reminder that proper calibration of a HFM is necessary when using

Diameter	Area	% of borehole area (BHA) allowing passing flow for the three diverter schemes and borehole sizes							
inches	Inches^2	Low	% BHA	Intermediate		% BHA	High		% BHA
4.0	12.56	1.31	**10.4**	2.91	A+F	**23.2**	6.84	A+K	**54.5**
5.5	23.75	1.31	**5.5**	4.62	A+B	**19.4**	10.37	A+G	**43.6**
6.0	28.27	1.31	**4.6**	7.83	A+B+C	**27.7**	14.02	A+G+H	**49.6**
			0.9			**8.3**			**6.0**
7.5	44.17	1.31	**3.0**	8.22	A+D	**18.6**	23.22	A+I	**52.6**
8.0	50.26	1.31	**2.6**	12.85	A+D+E	**25.6**	28.42	A+I+J	**56.5**
			0.4			**7.0**			**3.9**

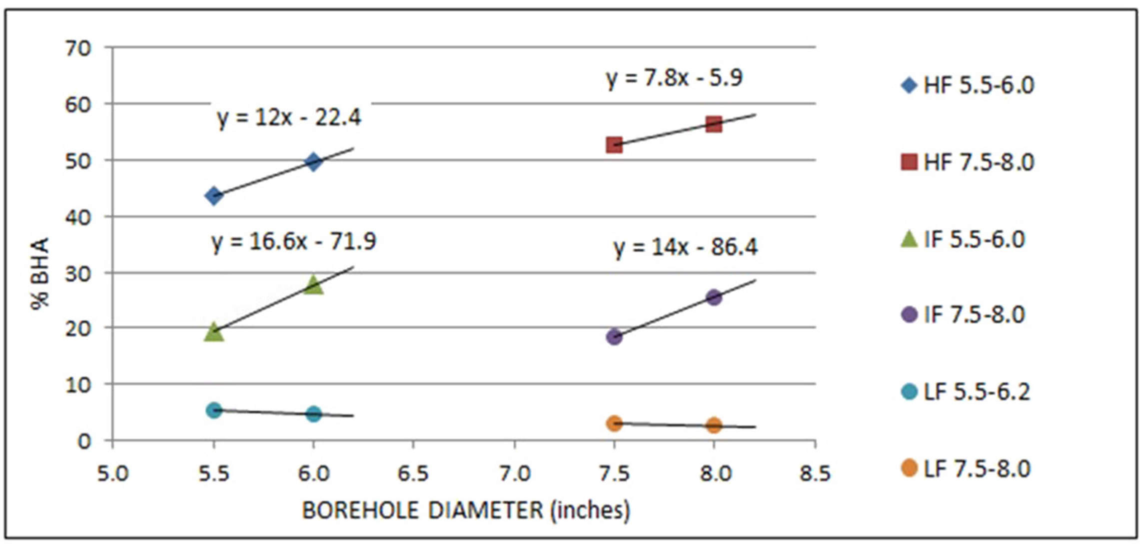

Figure 13: Table and accompanying chart detailing the relative percentages of passing flow provided by each diverter design diagrammed in Figure 11. Four (4) linear-regression equations were derived to quantify the changes in flow area accompanying small changes in borehole diameter, for example in going from a 5.5- to 6-inch diameter hole. Only those equations for the intermediate- and high-rate designs were incorporated into the MS- Excel flow calculator (Figure 14) because very small changes in area are noted in for the low-flow scheme whereas they vary up to ~8% for the passing-flow schemes.

Table 3: Comparison error summary of Mt. Sopris and NJGWS flow calculations versus controlled rates in a 5.5-inch diameter pipe

LOW FLOW MT SOPRIS DIVERTER WITH UPPER TRI-WING CENTRALIZER												
	UPWARD FLOW						DOWNWARD FLOW					
	Rate	**Time**	**NJGWS**		**Mt. Sopris**		**Rate**	**Time**	**NJGWS**		**Mt. Sopris**	
No.	gpm	Sec.	gpm	error	gpm	error	gpm	Secs	gpm	error	gpm	error
1	0.033	9.900	0.032	4.2	0.030	8.8	0.010	31.02	0.009	8.0	0.010	4.5
2	0.088	4.100	0.089	1.3	0.080	10.4	0.010	31.93	0.009	11.5	0.010	1.6
3	0.088	4.000	0.092	4.1	0.082	7.3	0.010	27.27	0.011	6.3	0.012	16.7
4	0.088	4.000	0.092	4.1	0.082	7.3	0.010	28.52	0.010	1.6	0.011	12.6
5	0.180	2.200	0.185	2.8	0.166	8.2	0.010	27.16	0.011	6.7	0.012	17.0
6	0.180	2.150	0.190	5.4	0.171	5.2	0.033	9.550	0.034	2.5	0.038	13.5
7	0.180	2.350	0.171	5.0	0.153	17.3	0.033	9.600	0.034	1.9	0.038	13.0
8	0.180	2.300	0.176	2.4	0.158	14.3	0.040	8.600	0.038	5.3	0.043	7.2
9	0.226	1.850	0.227	0.4	0.206	9.5	0.040	8.400	0.039	2.6	0.044	9.7
10	0.226	1.880	0.223	1.5	0.202	11.7	0.040	8.150	0.040	0.7	0.046	12.8
11	0.226	1.950	0.213	5.9	0.193	17.0	0.040	8.250	0.040	0.6	0.045	11.6
12							0.102	3.450	0.104	1.7	0.135	24.3
13							0.102	3.500	0.102	0.1	0.132	22.8
14							0.102	3.550	0.101	1.5	0.130	21.4
15							0.102	3.500	0.102	0.1	0.132	22.8
16							0.130	2.700	0.136	4.3	0.188	31.0
17							0.130	2.750	0.133	2.3	0.184	29.2
18							0.130	2.750	0.133	2.3	0.184	29.2
19							0.330	1.250	0.317	4.2	0.594	44.4
20							0.330	1.200	0.331	0.4	0.634	47.9
21							0.330	1.250	0.317	4.2	0.594	44.4
			AVG	**3.4**		**9.7**			**AVG**	**3.3**		**20.8**

one to determine aquifer transmissivity (Day-Lewis and others, 2011), because using inappropriate IRT-to-flow reference curves will produce inaccurate results. The MatrixHeat polynomial solution is only reliable for use at low-flow rates in ~6-inch diameter boreholes. Calculated flow rates for the 5.5-inch pipe (Figure 12A) cluster nicely along a single reference curve except in the case of downward flows where we begin see small time-lag effects, perhaps from countering upward-convection as a heat-pulse tends to rise in a sub vertical fluid column. Although the derived accuracy error for the ~6-inch well is ~12% at about 2 gpm, the value for a ~8-inch-diameter well at a similar rate is about three times that (~36%). It is important to note that as currently built, the caliper facture for the ~8-inch wells is inverted with respect to the ~6-inch ones because as Figure 3 shows, the relationships for small-to-larger diameter wells with respect to the observed flow rates is reversed; that is, calculated flow rates increase with an increase in borehole diameter for the smaller wells but decreases for the larger ones. We therefore multiplied the power solutions by the caliper factor for the smaller wells, but divided the power solution by the caliper for the larger ones. This approach is considered preliminary with the hope of future refinement and improvement from more field deployment and further laboratory testing. The error analysis summarized in Table 5 emphasizes the magnitude of errors that can arise when deploying the tool in the custom, passing-flow mode, especially for the larger-diameter wells.

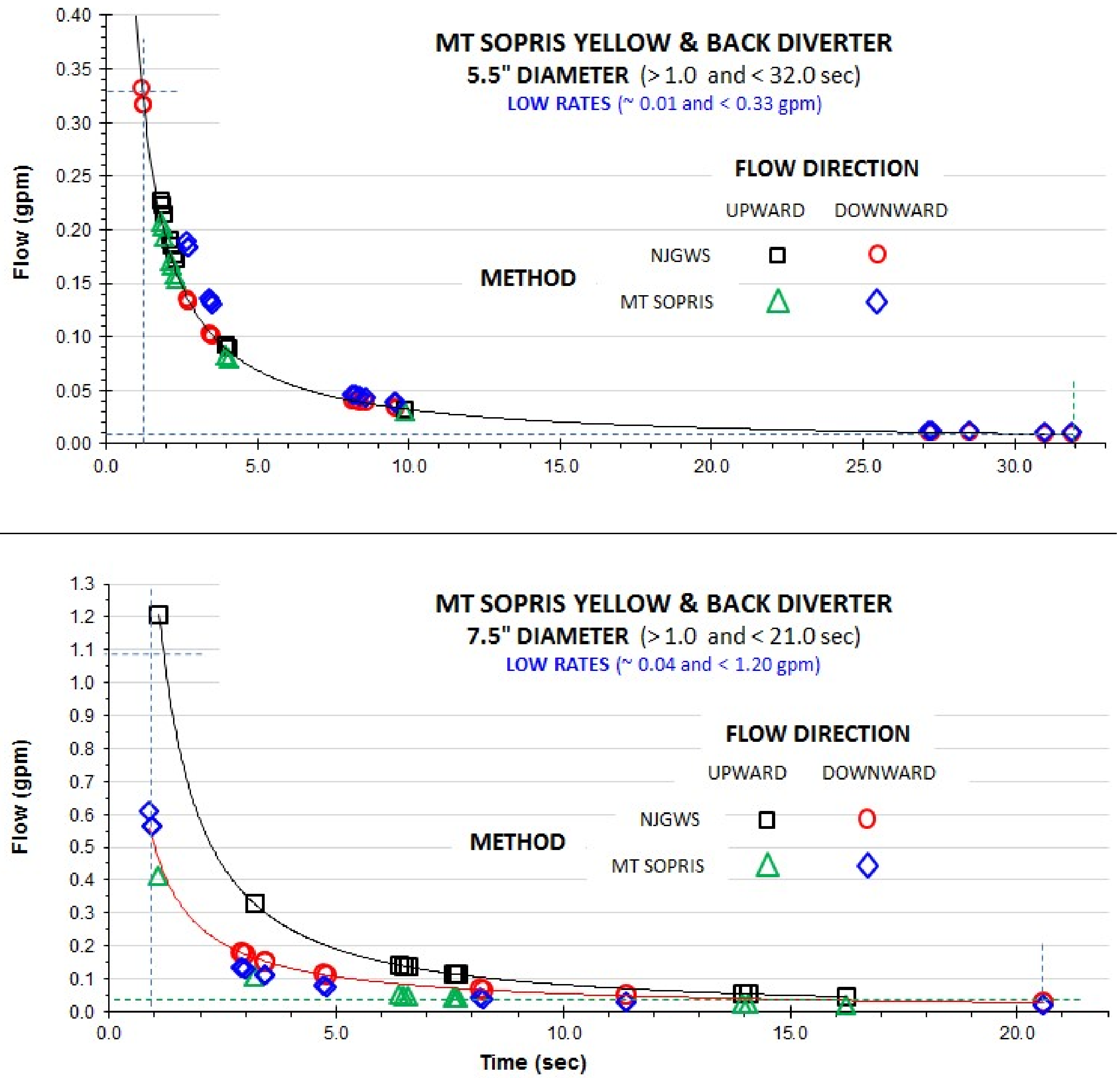

Figure 14: MS Excel charts comparing calculated flow rates in the 5.5- and 7.5inch-dimater pipes using the power solutions derived here versus the Mt. Sopris solution included in the current revision of the MatrixHeat software. Calculated values for the 5.5-inch pipe (A) cluster nicely along a single reference curve except in the case of downward flows where we begin see small lag effects for downward flows, perhaps from countering the upward-directed effects of heat-pulse that convection in a sub vertical fluid column. Chart B shows that the MatrixHeat solution that is calibrated for use in 6-inch holes consistently underestimates flow in the ~8-inch holes and by a large margin for upward cross flows.

Table 4: Comparative flow rates at different IRTs with summary of percentage differences between downward and upward axial flows in the 2 to 32 second time window calculated using the derived power equations of Table 1.

HFR5.5	Calculated		
sec	down	up	% DIFF
2	4.068425	4.363137	-7.2
4	2.805913	2.730879	2.7
6	2.257820	2.076179	8.0
8	1.935184	1.709253	11.7
14	1.433685	1.170880	18.3
20	1.184203	0.920023	22.3
26	1.028851	0.770501	25.1
32	0.920488	0.669597	27.3
		AVG =	**14.3**

HFR7.5	Calculated		
sec	down	up	% DIFF
2	7.686776	10.41010	-35.4
4	5.228433	6.037335	-15.5
6	4.173158	4.389728	-5.2
8	3.556304	3.501352	1.5
14	2.605372	2.255318	13.4
20	2.136703	1.703942	20.3
26	1.846680	1.386422	24.9
32	1.645332	1.177651	28.4
		AVG =	**17.4**

IFR5.5	Calculated		
sec	down	up	% DIFF
2	1.379139	1.512160	-9.6
4	0.834953	0.869110	-4.1
6	0.622547	0.628605	-1.0
8	0.505495	0.499519	1.2
14	0.337099	0.319422	5.2
20	0.260380	0.240214	7.7
26	0.215334	0.194786	9.5
32	0.185279	0.165008	10.9
		AVG =	**6.2**

IFR7.5	Calculated		
sec	down	up	% DIFF
2	2.309996	2.756498	-19.3
4	1.587647	1.512397	4.7
6	1.274937	1.064561	16.5
8	1.091181	0.829801	24.0
14	0.806145	0.511096	36.6
20	0.664678	0.375282	43.5
26	0.576724	0.299008	48.2
32	0.515445	0.249798	51.5
		AVG =	**28.5**

LF5.5	Calculated		
sec	down	up	% DIFF
2	0.189201	0.206970	-9.4
4	0.088388	0.091727	-3.8
6	0.056630	0.056986	-0.6
8	0.041292	0.040653	1.5
14	0.022336	0.021075	5.6
20	0.015098	0.013865	8.2
26	0.011319	0.010189	10.0
32	0.009012	0.007985	11.4
		AVG =	**6.3**

LF7.5	Calculated		
sec	down	up	% DIFF
2	2.575736	2.756498	-7.0
4	1.319494	1.512397	-14.6
6	0.892235	1.064561	-19.3
8	0.675948	0.829801	-22.8
14	0.393896	0.511096	-29.8
20	0.279191	0.375282	-34.4
26	0.216743	0.299008	-38.0
32	0.177389	0.249798	-40.8
		AVG =	**25.8**

Table 5: Example results calculated using the MS Excel flow-calculator with some field-test results from 2011 (Figure 3) taken at high rates of flow when using the high-rate bypass diverter.

High rate of upward flow in a 5.5 to 6.2-inch diameter well								
CALIPER (in)	TIME (s)	$OFR_{6.0}$	$CFR_{5.5}$	ERR1%	$CAL_{5.5to6.2}$	AFR	**ERR2%**	PFA%
6	9.6	2.25	1.52	32.3	1.14	1.73	**12.1**	49.6
High rate of upward flow in a 7.5 to 8.2-inch diameter well								
CALIPER (in)	TIME (s)	$OFR_{8.0}$	$CFR_{7.5}$	ERR3%	$CAL_{7.5to8.2}$	AFR	**ERR4%**	PFA%
8	11	1.87	2.73	-45.8	1.07	2.54	**-35.7**	56.5

OFR-Observed flow rate (gpm), CFR-calculated flow rate (either for 5.5- or 7.7-inch hole in gpm), CAL-Caliper factor, PFA-Percentage passing flow area relative to borehole cross-section area

A somewhat vexing aspect of deploying a HFM system can be the equalization process. This is the routine preceding release of a heat pulse into the water column. During this routine, the system operator monitors a visual display of a line that continuously charts the amplitude of the response curve determined from heat-sensor readings provided by the two thermistors over a period of time. The ideal equalization curve is stable and flat over a prolonged period, from over a dozen seconds to minutes if necessary, before firing a heat pulse and registering the IRT. From our experience, if there are transient pumping effects in the area of the borehole being tested, or in the case of the laboratory test, transient fluctuations in the water pressure in the supply line, equalization does not return a stabilized signal but can fluctuate and periodically spike rather than returning a stable signal indicating stabilized cross flows (Figure 2). During the laboratory tests we also sometimes observed equalization curves that rhythmically fluctuated as low-frequency sinusoidal curves that compromised acquisition of test data at certain flow rates and that probably reflect flow-regime changes at various combinations of pipe diameter and flow rate. This is an interesting aspect of these tests that merits further work in order to understand this phenomenon more thoroughly.

Following are three some operational tips that we have learned from deploying our HFM systems that may be helpful when deploying yours:

1) Cross-flow rates can vary in direction and magnitude relative to nearby topographic and structural geological conditions (Herman, 2014). In many cases, directions of cross flows can be reasonably estimated before logging by first constructing a simple hydrogeological profile that includes the topographic grade, structural attitude of geological strata, and the well-construction information including the total depth of the well, the depth of casing, and the penetrated, open stratigraphic interval. And knowing the depth of permeable geological features before HFM testing can be useful and save deployment time. Many examples of more thoroughly developed profiles are available for various fractured-bedrock aquifers in New Jersey that exemplify these concepts (Herman, 2010; Herman and Curran, 2010).

2) Cross-flow rates vary drastically in different aquifer systems, with solution-prone ones like dolomite and limestone typically having the highest measured rates (Herman and Curran, 2014)

3) Transient pumping effects depend on standard water-use cycles that peak during the early morning, mid-day, and late afternoon times during low-flow testing.

As a final note, we set out to test our HFM system with the intent of refining its operational range and therefore its potential use. As is typical with testing of scientific instrumentation, the facilities needed for testing and the amount of time required to fully understand their operational thresholds and precision is

NJ GEOLOGICAL & WATER SURVEY FLOW CALCULATOR FOR A HPFM 2293

5.5 to 6.2-inch Diameter Boreholes

FLOW RATE & DIRECTION	FLOW RANGE GPM	TIME RANGE seconds	CALIPER inches	TIME seconds	FLOW GPM
LOW UP	> .01 < 0.4	> 1.8 < 32.0		5.3	0.066
LOW DOWN	> .01 < 0.4	> 1.8 < 32.0		20.0	0.015
INTER UP	> 0.2 < 2.0	> 1.5 < 42.0	6.0	20.0	0.34
INTER DOWN	> 0.2 < 2.0	> 1.5 < 42.0	6.0	20.0	0.37
HIGH UP	> 0.9 < 7.0	> 1.0 < 24.0	6.0	20.0	1.06
HIGH DOWN	> 0.9 < 7.0	> 1.0 < 24.0	6.0	20.0	1.35

7.5 to 8.2-inch Diameter Boreholes

FLOW RATE & DIRECTION	FLOW RANGE GPM	TIME RANGE seconds	CALIPER inches	TIME seconds	FLOW GPM
LOW UP	> .02 < 1.0	> 0.9 < 21.0		10.0	0.082
LOW DOWN	> .02 < 1.0	> 0.9 < 21.0		10.0	0.054
INTER UP	> 0.3 < 3.0	> 1.5 < 32.0	8.0	10.0	0.94
INTER DOWN	> 0.3 < 3.0	> 1.5 < 32.0	8.0	10.0	1.33
HIGH UP	> 1.5 < 8.0	> 1.5 < 41.0	8.0	10.0	2.74
HIGH DOWN	> 1.5 < 8.0	> 1.5 < 41.0	8.0	10.0	2.92

Rev. 02/2015

Method for using a caliper function for refining calculated flow rates in variable-diameter boreholes when using the PFA diverter schemes

Figure 15: A screen-captured image of the NJGWS MS Excel flow calculator used with a HFP-2293. Two sheets provide IRT to flow-rate calculates for ~6 to 8 inch wells when using three diverter schemes covering low-, intermediate-, and high-flow ranges. Photographs summarize the respective deployment schemes.

ordinarily cost prohibitive, and in this case benefits from the voluntary research reported here. This technology is relatively new and rapidly evolving, sometime in parallel, with competing technologies that may someday render HFM technology obsolete. But for now, these instruments are gaining a foothold in the industry to aid with groundwater-pollution investigations in response to regulatory oversight. They currently are not required to be certified for use, nor are their operators. We therefore simply continue to refine our geophysical toolkit used to characterize complex, fractured-rock aquifers that benefit from knowing the rates and directions of groundwater cross flow in open boreholes.

Acknowledgments

We thank Ms. Bay Weber of the Stony Brook-Millstone Watershed Association for site access to use their well field in Hopewell Township. We thank John Curran, Steve Spayd, Gregg Steidl, Mike Gagliano, Michelle Kuhn, Ray Bousenberry, Ted Pallis and Brian Buttari of the NJGWS Geological Research and Support Section for approval, contributing advice and providing constructive feedback during this work and for contributing to a productive atmosphere of cooperation and teamwork. James T. Boyle, Chief of the NJGWS Groundwater Supply and Analysis section, and pictured on the report cover, proved valuable suggestions implemented during the tests. We thank Jim Peterson and Princeton Geosciences, Inc., for use of their HFM during testing, and providing a scientific review of this work during report editing and production. We thank Tenika Haywood for helping procure the test equipment. We also thank Jim Lococo of Mt. Sopris Instrument Company for reviewing and providing comments on this work. Jeff Hoffman of the NJGWS permitted us to publish this through GANJ to expedite its release for use. Accordingly, Suzanne Macaoaoy-Ferguson helped proof and format the article

References

Herman, G. C., 2010, Hydrogeology and borehole geophysics of fractured-bedrock aquifers, Newark Basin, New Jersey (5 MB PDF), in Herman, G. C., and Serfes, M. E., eds., Contributions to the geology and hydrogeology of the Newark basin: N.J. Geological Survey Bulletin 77, Chapter F., p. F1-F45.

Herman, G. C., 2006, Field Tests Using a Heat-Pulse Flow Meter to Determine its Accuracy for Flow Measurements in Bedrock Wells (2 MB PDF): New Jersey Geological Survey Technical Memorandum TM06-1, 8 p.

Herman, G. C., 2006 Hydrogeological framework of the Brunswick aquifer at Heron Glen Golf Course, Hunterdon County, New Jersey Geological Survey Newsletter Vol 2., No. 1, Winter 2006, p. 8-11. Herman, 2012.

Herman, G. C. and Curran, John, 2010, Borehole geophysics and hydrogeology studies in the Newark basin, New Jersey (38 MB PDF), in Herman, G. C., and Serfes, M. E., eds., Contributions to the geology and hydrogeology of the Newark basin: N.J. Geological Survey Bulletin 77, Appendixes 1-4, 245 p.

Hess, A.E., 1986, identifying hydraulically-conductive fractures with a low-velocity borehole flowmeter: Canadian Geotechnical Journal, v. 23, no. 1, p. 69-78.

Day-Lewis, F.D., Johnson, C. D., Paillet, F.L., and Halford, K.J., 2011, A computer program for flow-log analysis of single holes (FLASH): Ground Water, doi: 10.1111/j.1745-6584.2011.00798.x

Hess, A.E., and Paillet, F.L., 1990, Applications of the thermal-pulse flowmeter in the hydraulic characterization of fractured rocks: American Society for Testing Materials, ASTM STP 101, p. 99-112.

Paillet, F.L., 1998, Flow modeling and permeability estimation using borehole flow logs in heterogeneous fractured formations: Water Resources Research, vol. 34, no. 5, p. 997-1010.

National Research Council Committee on Fracture Characterization and Fluid Flow, 1996, Rock Fractures and Fluid Flow: Contemporary Understanding and Applications: National Academy Press, Washington, D.C., 568 pages

New Jersey Department of Environmental Protection, 2012, Ground Water Technical Guidance: Site Investigation, Remedial Investigation, and Remedial Action Performance Monitoring. http://www.state.nj.us/dep/srp/srra/training/sessions/gw_overview.pdf

New Jersey Department of Environmental Protection, 2005, Field sampling procedures manual, URL: http://www.nj.gov/dep/srp/guidance/fspm/.

Appendix A

Tables of laboratory testing of the Mt. Sopris HFP-2293 under varying flow conditions

Table A1: Low-flow test, Mt. Sopris yellow-and-black diverter in a 5.5-inch diameter pipe

	UPWARD		$y = 6.419x^{-0.640}$		**DOWNWARD**		$y = 5.899x^{-0.536}$	
ID	Rate gpm	Time (x) secs.	Calculated (y) gpm	Error %	Rate gpm	Time (x) secs.	Calculated (y) gpm	Error %
1	0.033	9.900	0.032	3.5	0.010	31.020	0.009	7.4
2	0.088	4.100	0.090	1.9	0.010	31.930	0.009	11.4
3	0.088	4.000	0.092	4.9	0.010	27.270	0.011	5.4
4	0.088	4.000	0.092	4.9	0.010	28.520	0.010	0.3
5	0.180	2.200	0.186	3.5	0.010	27.160	0.011	5.9
6	0.180	2.150	0.191	6.3	0.033	9.550	0.033	0.0
7	0.180	2.350	0.172	4.2	0.033	9.600	0.033	0.7
8	0.180	2.300	0.177	1.8	0.040	8.600	0.038	6.2
9	0.226	1.850	0.228	1.0	0.040	8.400	0.038	3.8
10	0.226	1.880	0.224	0.9	0.040	8.150	0.040	0.5
11	0.226	1.950	0.215	5.1	0.040	8.250	0.039	1.8
12					0.102	3.450	0.102	0.4
13					0.102	3.500	0.101	1.1
14					0.102	3.550	0.099	2.7
15					0.102	3.500	0.101	1.1
16					0.130	2.700	0.134	3.2
17					0.130	2.750	0.131	1.1
18					0.130	2.750	0.131	1.1
19					0.330	1.250	0.313	5.2
20					0.330	1.200	0.327	0.8
21					0.330	1.250	0.313	5.2
			AVERAGE	**3.4**				**3.1**

Table A2: Low-flow test, Mt. Sopris yellow-and-black diverter in a 7.5-inch diameter pipe

	UPWARD		$y = 17.95x^{-0.786}$		DOWNWARD		$y = 11.301x^{-0.556}$	
ID	Rate	Time (x)	Calculated (y)	Error	Rate	Time (x)	Calculated (y)	Error
	gpm	secs.	gpm	%	gpm	secs.	gpm	%
1	0.039	13.950	0.054	39.5	0.026	20.600	0.027	2.8
2	0.039	14.100	0.054	37.7	0.026	20.600	0.027	2.8
3	0.039	16.250	0.045	15.8	0.048	11.400	0.048	0.1
4	0.123	7.600	0.114	7.2	0.048	11.400	0.048	0.1
5	0.123	7.650	0.113	7.9	0.068	8.250	0.066	3.5
6	0.123	7.700	0.112	8.6	0.068	8.200	0.066	2.9
7	0.200	6.400	0.141	29.6	0.110	4.750	0.112	1.6
8	0.200	6.500	0.138	30.9	0.110	4.800	0.111	0.6
9	0.200	6.600	0.136	32.2	0.150	3.450	0.152	1.5
10	0.290	3.200	0.328	13.1	0.150	3.450	0.152	1.5
11	0.290	3.200	0.328	13.1	0.150	3.450	0.152	1.5
12	0.290	3.200	0.328	13.1	0.184	2.950	0.177	3.8
13	1.000	1.100	1.207	20.7	0.184	2.900	0.180	2.2
14					0.184	3.000	0.174	5.3
15					0.528	0.900	0.557	5.4
16					0.528	0.950	0.528	0.1
17					0.528	0.950	0.528	0.1
			AVERAGE	**20.7**				**2.1**

Table A3: Intermediate flow test, NJGWS custom diverter 1 in a 5.5-inch diameter pipe

	UPWARD		$y = 2.631x^{-0.799}$		DOWNWARD		$y = 2.278x^{-0.724}$	
ID	Rate	Time (x)	Calculated	Error	Rate	Time (x)	Calculated (y)	Error
	gpm	secs.	gpm	%	gpm	secs.	gpm	%
1	_0.26*_	_16.90_	0.27	7.3	_0.15_	_40.45_	0.16	7.8
2	_0.26_	_17.25_	0.27	5.6	_0.15_	_41.02_	0.15	4.6
3	_0.26_	_16.90_	0.27	7.3	_0.15_	_40.57_	0.15	5.5
4	0.45	9.65	0.43	4.4	0.25	20.60	0.25	0.3
5	0.45	9.75	0.43	5.2	0.25	21.14	0.24	2.2
6	0.45	9.65	0.43	4.4	0.25	20.60	0.25	0.3
7	0.49	8.50	0.48	2.9	0.25	20.39	0.25	0.4
8	0.49	8.20	0.49	0.0	_0.27_	_21.75_	0.24	9.6
9	0.49	8.00	0.50	1.9	_0.27_	_20.65_	0.25	6.1
10	_0.60_	_6.60_	0.58	2.9	_0.27_	_21.20_	0.24	7.9
11	_0.60_	_6.55_	0.59	2.3	0.27	25.90	0.21	21.8
12	_0.60_	_6.65_	0.58	3.5	0.27	24.16	0.22	17.7
13	0.81	4.45	0.80	1.5	0.27	24.35	0.22	18.2
14	0.81	4.55	0.78	3.2	0.27	24.68	0.22	19.0
15	0.81	4.80	0.75	7.2	_0.47_	_6.80_	0.55	17.7
16	0.90	3.95	0.88	2.5	_0.47_	_7.30_	0.53	11.9
17	0.90	3.90	0.89	1.5	_0.47_	_6.65_	0.56	19.6
18	0.90	3.90	0.89	1.5	_0.47_	_6.75_	0.56	18.4
19	1.08	3.00	1.09	1.3	0.47	8.05	0.49	4.3
20	1.08	3.05	1.08	0.1	0.47	7.85	0.50	6.2
21	1.08	3.05	1.08	0.1	0.47	7.95	0.49	5.2
22	_1.15_	_2.65_	1.21	5.0	0.47	7.75	0.50	7.2
23	_1.15_	_2.65_	1.21	5.0	0.67	5.05	0.69	2.3
24	_1.15_	_2.65_	1.21	5.0	0.67	5.05	0.69	2.3
25	1.34	2.25	1.38	2.7	0.67	5.05	0.69	2.3
26	1.34	2.35	1.33	0.8	0.67	5.15	0.68	0.9
27	1.34	2.30	1.35	0.9	0.85	4.00	0.81	4.6
28	_1.72_	_1.70_	1.72	0.1	0.85	4.05	0.80	5.5
29	_1.72_	_1.70_	1.72	0.1	0.85	4.05	0.80	5.5
30	_1.72_	_1.70_	1.72	0.1	0.85	4.10	0.80	6.3
31	1.95	1.45	1.96	0.3	1.00	2.95	1.01	1.0
32	1.95	1.45	1.96	0.3	1.00	2.95	1.01	1.0
33	1.95	1.45	1.96	0.3	1.00	2.95	1.01	1.0
34	_2.20_	_1.25_	2.20	0.1	1.00	2.95	1.01	1.0
35	_2.20_	_1.25_	2.20	0.1	_1.83_	_2.08_	1.30	29.0
36	_2.20_	_1.25_	2.20	0.1	_1.83_	_1.69_	1.51	17.6
37					_1.83_	_1.70_	1.50	18.0
			AVERAGE	**2.4**				**8.4**

*_Italicized font for NJGWS Model HFP-2293HFM_
Regular font for Princeton Geosciences, LLC Model HFP-2293 HFM

Table A4: Intermediate flow, NJGWS custom diverter 1 in a 7.5-inch diameter pipe

	UPWARD		$y = 5.024x^{-0.866}$		DOWNWARD		$y = 3.361x^{-0.541}$	
ID	Rate	Time (x)	Calculated (y)	Error	Rate	Time (x)	Calculated (y)	Error
	gpm	Seconds	gpm	%	gpm	Seconds	gpm	%
1	*0.26**	*27.70*	*0.28*	*8.4*	*0.54*	*31.49*	*0.52*	*3.7*
2	*0.26*	*27.65*	*0.28*	*8.6*	*0.54*	*30.35*	*0.53*	*1.8*
3	*0.26*	*27.00*	*0.29*	*10.9*	*0.54*	*31.80*	*0.52*	*4.3*
4	0.32	22.13	0.34	6.4	0.67	19.50	0.67	1.0
5	0.32	23.38	0.33	1.4	0.67	19.40	0.68	1.3
6	0.32	22.43	0.34	5.1	0.67	19.29	0.68	1.6
7	*0.62*	*12.35*	*0.57*	*8.1*	*1.09*	*7.55*	*1.13*	*3.3*
8	*0.62*	*12.20*	*0.57*	*7.1*	*1.09*	*7.31*	*1.15*	*5.1*
9	*0.62*	*12.70*	*0.55*	*10.3*	*1.09*	*7.45*	*1.13*	*4.0*
10	*0.62*	*12.55*	*0.56*	*9.4*	1.20	6.75	1.20	0.3
11	*1.09*	*6.20*	*1.03*	*5.3*	1.20	6.65	1.21	0.5
12	*1.09*	*6.10*	*1.05*	*4.0*	1.20	6.45	1.23	2.1
13	*1.09*	*5.80*	*1.09*	*0.3*	*1.34*	*5.25*	*1.37*	*2.2*
14	*1.09*	*6.65*	*0.97*	*10.9*	*1.34*	*5.35*	*1.36*	*1.2*
15	1.47	4.70	1.31	10.7	*1.34*	*5.30*	*1.36*	*1.7*
16	1.47	4.70	1.31	10.7	1.78	3.40	1.73	2.6
17	*1.51*	*3.95*	*1.53*	*1.0*	1.78	3.45	1.72	3.4
18	*1.51*	*3.90*	*1.54*	*2.2*	1.78	3.40	1.73	2.6
19	*1.51*	*3.80*	*1.58*	*4.5*	*1.82*	*2.95*	*1.87*	*2.8*
20	*1.51*	*3.85*	*1.56*	*3.3*	*1.82*	*3.30*	*1.76*	*3.2*
21	*2.23*	*2.30*	*2.44*	*9.3*	*1.82*	*3.30*	*1.76*	*3.2*
22	*2.23*	*2.35*	*2.39*	*7.3*	*1.82*	*3.30*	*1.76*	*3.2*
23	*2.23*	*2.25*	*2.49*	*11.4*				
24	2.34	2.45	2.31	1.4				
25	2.34	2.40	2.35	0.4				
26	2.34	2.55	2.23	4.7				
27	2.34	2.75	2.09	10.8				
28	2.34	2.65	2.16	7.8				
29	*2.88*	*1.70*	*3.17*	*10.0*				
30	*2.88*	*1.75*	*3.09*	*7.3*				
31	*2.88*	*1.80*	*3.02*	*4.7*				
			AVERAGE	**6.6**				**2.5**

Italicized font for NJGWS sonde,
Regular font for Princeton Geosciences, Inc. sonde

Table A5: High flow, NJGWS custom diverter 2 in a 5.5-inch diameter pipe

	UPWARD		$y = 6.419x^{-0.640}$		**DOWNWARD**		$y = 5.899x^{-0.536}$	
ID	Rate	Time (x)	Calculated (y)	Error	Rate	Time (x)	Calculated (y)	Error
	gpm	seconds	gpm	%	gpm	seconds	gpm	%
1	0.86	22.90	0.84	2.4	1.36	15.40	1.36	0.0
2	0.86	23.10	0.83	3.0	1.36	17.09	1.29	5.4
3	0.86	23.25	0.83	3.4	1.36	13.85	1.44	5.9
4	0.86	23.44	0.83	3.9	1.36	15.75	1.34	1.2
5	0.86	22.90	0.84	2.4	3.50	2.53	3.58	2.3
6	1.00	19.16	0.95	5.3	3.50	2.44	3.65	4.3
7	1.00	19.16	0.95	5.3	3.50	2.53	3.58	2.3
8	1.00	19.00	0.95	4.8	4.68	1.80	4.30	8.2
9	1.00	19.16	0.95	5.3				
10	1.54	8.35	1.66	7.8				
11	1.54	8.80	1.60	4.0				
12	1.54	9.10	1.57	1.7				
13	1.54	9.00	1.58	2.5				
14	2.50	4.15	2.66	6.5				
15	2.50	4.25	2.62	4.8				
16	2.50	4.25	2.62	4.8				
17	3.33	2.75	3.52	5.6				
18	3.33	2.70	3.56	7.0				
19	3.33	2.70	3.56	7.0				
20	4.70	1.80	4.68	0.3				
21	4.70	1.80	4.68	0.3				
22	4.70	1.80	4.68	0.3				
23	6.90	1.15	6.34	8.1				
24	6.90	1.15	6.34	8.1				
25	6.90	1.15	6.34	8.1				
			AVERAGE	**4.5**				**3.7**

Table A6: High flow, NJGWS custom diverter 2 in a 7.5-inch diameter pipe

	UPWARD				DOWNWARD			
ID	Rate	Time (x)	Calculated (y)	Error	Rate	Time (x)	Calculated (y)	Error
	gpm	seconds	gpm	%	gpm	seconds	gpm	%
1	1.72	16.80	1.95	13.6	1.50	40.10	1.45	3.2
2	1.72	17.75	1.87	8.8	1.50	38.73	1.48	1.4
3	1.72	18.70	1.80	4.4	1.50	32.60	1.63	8.6
4	1.72	20.70	1.66	3.6	1.50	35.14	1.56	4.1
5	1.72	23.95	1.48	14.0	1.87	31.25	1.67	10.8
6	1.72	16.65	1.97	14.4	1.87	31.49	1.66	11.2
7	2.50	14.08	2.25	10.2	1.87	31.17	1.67	10.7
8	2.50	13.56	2.31	7.5	2.30	14.70	2.54	10.2
9	2.50	13.25	2.36	5.8	2.30	17.05	2.33	1.5
10	3.40	7.70	3.61	6.1	2.30	16.30	2.39	4.1
11	3.40	7.80	3.57	5.1	2.30	17.85	2.28	1.0
12	5.80	3.83	6.25	7.7	2.30	17.55	2.30	0.1
13	5.80	4.20	5.81	0.2	2.88	11.01	2.98	3.4
14	5.80	3.75	6.35	9.5	2.88	11.10	2.96	2.9
15	5.80	4.30	5.70	1.7	2.88	10.50	3.06	6.2
16	5.80	4.00	6.04	4.1	3.26	8.25	3.50	7.2
17	6.70	4.25	5.76	14.1	3.26	7.80	3.61	10.6
18	6.70	3.95	6.10	9.0	3.26	8.13	3.52	8.1
19	6.70	3.56	6.62	1.2	3.26	8.20	3.51	7.6
20	6.70	3.40	6.86	2.4	5.35	4.30	5.02	6.1
21	6.70	3.65	6.49	3.2	5.35	4.15	5.12	4.3
22					5.35	3.35	5.77	7.9
23					5.35	4.50	4.90	8.5
24					5.35	4.00	5.23	2.3
25					6.25	2.60	6.64	6.3
26					6.25	2.80	6.38	2.0
27					6.25	3.15	5.97	4.5
28					6.25	2.90	6.25	0.0
29					6.52	3.00	6.14	5.9
30					6.52	3.10	6.02	7.6
31					6.52	2.75	6.44	1.2
32					6.52	3.05	6.08	6.8
			AVERAGE	**7.0**				**5.5**